



---

Unnið fyrir Innviðaráðuneytið

# Flugmælingar og úttekt á loftkviku yfir Hvassahrauni

Verkefnistími: janúar 2021 – mars 2024

Verkefnisstjórar:

Gylfi Árnason

Þorgeir Pálsson

Ólafur Rögnvaldsson

Sæmundur E. Þorsteinsson

Mars 2024



## Formáli

Meðfylgjandi skýrsla er lokaskýrsla um verkefni, sem unnið var samkvæmt samningi Háskólans í Reykjavík við Innviðaráðuneytið um mælingar og rannsóknir á loftkviku yfir Hvassahrauni, sem gerður var 31. des 2020 og var til tveggja ára þ.e. til ársloka 2022. Gert var ráð fyrir að fyrsta árið yrði forverkefni til að þróa og prófa þá mælitækni og úrvinnsluaðferðir, sem fýsilegast væri að beita við söfnun rannsóknargagna. Skýrslu um þetta forverkefni var skilað í nóvember 2021. Í lok árs 2022 var ákveðið að framlengja verkefnistímam um allt að einu ári vegna þess að verkefnið varð umfangsmeyra en áður hafði verið ætlað auk þess að tengjast öðrum verkefnum varðandi veðurfar á svæðinu.

Auk verkefnisstjórnanna, sem eru aðalhöfundar að þessari skýrslu, tók Jóhannes Bergur Gunnarsson, verkfræðingur og kennari við HR, sem vann að þróun og prófun mælibúnaðarins og framkvæmd mælinga í lofti auk þess að halda utan um útgáfu þessarar skýrslu. Þá tóku tveir verkfræðinemar við HR stóran þátt í framkvæmdinni, þeir Orri Steinn Guðfinnsson, og Freyr Hlynsson, sem þróuðu hugbúnað til hvers konar úrvinnslu og prófana á mæligögnum auk hermunar á eiginleikum þeirra. Kristján Orri Magnússon, flugmaður og tæknifræðingur vann að flugrekstrartæknilegum atriðum og túlkun á niðurstöðum mælinga auk skipulagningar verkferla. Ragnheiður Garðarsdóttir, verkfræðinemi við Embry-Riddle háskóla, og Jaan Jaerving tölvunarfræðingur við HÍ unnu að könnunum á að nota farsíma og farsímanet til að gera og skrá loftkvikumælingar í almennu flugi.

## Útdráttur

Í verkefninu er notaður hinn alþjóðlegi EDR mælikvarði til að lýsa styrkleika (ákefð) loftkviku, sem fundin er út frá mælingu á lóðréttri hröðun flugvélar. Jafnframt eru gerðar aðgengilegar myndir af styrkleika og svæðisbundinni dreifingu á loftkviku fyrir hverja mælingarflugferð með því að varpa mælingum eftir flugferli yfir í EDR hæðarlínukort fyrir svæðið í grennd við áætlað flugvallarsvæði. Að lokum voru þróuð svonefnd fylgnilíkön, sem bjóða upp á megindlegt mat á meðalgildi EDR í mismunandi flughæð innan hrings frá miðju flugvallar fyrir gefinn vindhraða og vindstefnu (*sjá kafla 2.4 í skýrslu HR-hópsins*). Þessi líkön gefa styrk loftkviku í EDR einingum í hverjum punkti á svæðinu við tilgreind vindskilyrði og má nota til að áætla styrk loftkviku á hugsanlegum flugferlum fyrir landingu eða brottflug. Lýst er greiningu á flugmælingum, sem gerðar hafa verið í þessu verkefni og fjallað er um í skýrslunni. Þær leiða í ljós að þær veðurastæður, sem líklega valda mestri loftkviku á svæðinu, er hvass vindur sem berst inn á svæðið úr stefnu á milli Austurs og Suðurs ( $80^\circ$  -  $180^\circ$ ). Vindur úr þessum áttum er því líklegastur til að valda aukinni loftkviku, hafa áhrif á flugöryggi og nothæfi flugvallar í Hvassahrauni. Samkvæmt því má draga þá ályktun að loftkvika, þegar EDR í núverandi veðurmastri er  $0.4 \text{ m}^{2/3}/\text{s}$  eða hærri, hamli flugi smærri flugvéla á Hvassahraunssvæðinu, en að loftkvika ein og sér (“severe turbulence”) muni ekki hamla að- eða fráflugi stærri flugvéla, eins og t.d. Dash 8. Hér ber þó að hafa í huga að flugmælingar á svæðinu hafa enn ekki verið gerðar fyrir meira en  $12 \text{ m/s}$  ( $25$  hnúta) vindstyrk.



## Table of Contents

1	Introduction .....	7
1.1	Background .....	7
1.2	Aviation Turbulence .....	7
1.3	Turbulence Metrics .....	8
1.4	Pilot Project of 2021 .....	9
1.5	Measurement Methods .....	9
1.6	Aircraft Response to Turbulence .....	9
1.7	Typical Measurement Mission .....	10
1.7.1	Track and data presented in Google Earth .....	10
1.7.2	Quality Control of Recorded Measurement Data .....	11
1.7.3	Measurement Data and EDR Contour Maps .....	12
2	Measurement Program at Hvassahraun Airport Site .....	15
2.1	Playing Area and Instrumentation .....	15
2.2	Weather Conditions of Interest .....	15
2.3	Measurement Methodology and Procedures .....	16
2.4	3D Presentation of EDR Measurements .....	16
2.4.1	Correlation of in-situ EDR Measurements with Met Mast .....	17
2.4.2	Correlation with Lidar Measurements .....	18
2.4.3	Correlation with Belgingur Wind Forecast .....	19
2.5	Network for Automated Collection and Processing of In-flight Measurement Data ....	20
3	Measurement Mission Reports .....	23
3.1	Aircraft Missions .....	23
3.2	Comparison of BIRK and HVH .....	26
4	Turbulence Conditions in Hvassahraun .....	29
4.1	EDR Contour Plots of Measurements .....	29
4.2	Case studies of Flight Segments .....	30
4.3	Grouping of flight segments under similar conditions .....	31
4.4	Correlation of flight segments under similar conditions .....	36
4.5	Comparison of Correlation Model and Independent Flight Results .....	38

4.6	Comparison of In-Flight and Mast Measurements .....	39
4.7	Comparison of in-Flight and Lidar Measurements .....	40
4.8	Overall assessment of Turbulence Conditions .....	42
4.9	Criteria to mark severe Turbulence .....	43
4.10	Anatomy of a severe turbulent event .....	47
4.11	Proposed use of correlations and variability statistics .....	48
5	Simulation of Aircraft Response to Typical Turbulence.....	51
5.1	Objectives of the Simulations .....	51
5.2	Simulation Tool for Turbulence Assessment .....	52
5.3	Response of Individual Aircraft types .....	53
5.3.1	Response of Light Measurement Aircraft .....	54
5.3.2	Response of Bombardier Dash 8 – 200.....	56
5.3.3	Response of Boeing 757-200 .....	58
5.3.4	Key Statistical Results of Type Simulation Tests .....	59
5.4	Comparative Response of Aircraft on a Fixed Course.....	61
5.5	Simulations of Aircraft Response to Turbulence - Summary of Result.....	63
6	Conclusions and Recommendations .....	65
6.1	Summary and Results .....	65
6.2	Main Conclusions .....	69
6.2.1	Turbulence frequency, strength, and geographic distribution.....	69
6.2.2	Weather influence of turbulence on airport safety and utilization .....	69
6.2.3	Comparison of Keflavik and Reykjavik Airports with Hvassahraun Site .....	69
6.2.4	Effect of turbulence on various types of aircraft.....	70
6.3	Recommendations.....	70
6.3.1	Further analyses and studies .....	70
6.3.2	Further research .....	70

# 1 Introduction

## 1.1 Background

Icelandic aviation authorities are considering building a new airport at Hvassahraun (midpoint approximately 64.01N, -22.11E), some 20 km SW from Reykjavik and for that reason have sponsored preparatory meteorological measurements for the site. Similar plans for a new airport (Kapelluhraun, 5 km from Hvassahraun) were evaluated in the late 1960's. One of the major issues raised at that time related to a perceived high level of aviation turbulence in the area especially if wind was coming from 80 to 210 degrees. Over two hundred observation flights were made for the purpose of evaluating the flight conditions in the area based on pilot assessment of the weather conditions experienced during these flights. No in-flight measurements were carried out so the results were qualitative as to the intensity and other characteristics of the turbulence encountered. Hence it was decided in 2019 that an estimation of the air turbulence in the area was required as a part of the overall preparatory work that needed to be undertaken for a comprehensive evaluation of the new airport site at Hvassahraun.

## 1.2 Aviation Turbulence

“Bumpiness” in flight, often referred to as aviation turbulence or simply turbulence, is caused by seemingly random movement of air (“eddies”) across the aircraft flight path. Light turbulence causes bumpiness which may bother some passengers but is not a threat to safe air travel. Extreme turbulence on the other hand can cause injury, loss of control or even breakup of the aircraft structure or parts thereof. The intensity of “bumpiness” depends on the magnitude and size of the encountered atmospheric turbulent eddies as well as the aircraft response to those eddies. Traditional pilot reports (PIREP) have typically classified turbulence as light, moderate, severe and extreme. PIREPs have been used to mark areas of unusual turbulence and often enabled pilots (supported by air traffic controllers) to avoid turbulence encounters, and thereby improve safety and comfort.

Turbulence has been classified according to the nature of the atmospheric disturbance. Clear air turbulence (CAT) refers to “all turbulence in the free atmosphere of interest in aerospace operations that is not adjacent to visible convective activity”. This occurs primarily at cruising altitudes (10 km).

Turbulence associated with the large amplitude gravity waves and breaking gravity waves (which can extend to very high levels, through the troposphere, and into the stratosphere and beyond) above and behind mountainous terrain in stably stratified flow is often termed mountain wave turbulence (MWT). Typically, stable gravity waves consist of smooth laminar wind flows which are accompanied by strong, erratic and highly turbulent rotating eddies which are located at lower levels often under the peaks of the waves and may also be generated by break-up of the wave structure.

Convective turbulence is associated with strong updrafts and downdrafts in dry thermals or convective clouds most often caused by solar heating of the earth's surface under unstable atmospheric conditions. Turbulence associated with convective clouds (either in-cloud or near-cloud) is collectively termed convectively induced turbulence or CIT.

Low-level turbulence (LLT), which is of primary interest at Hvassahraun, results from convection and strong winds associated with surface frontal passages, dry thermals during the daytime over hot surfaces, and mechanical forcing associated with flow over surface obstacles (mountains and hills with lee side eddy separation, trees, buildings) or rough flat terrain. Its intensity is determined by low-level wind speed, stability of the air mass, height above the ground, and terrain. This source of turbulence is typically within the planetary boundary layer and can be a significant safety hazard during takeoffs and landings, especially for small aircraft. This is the type of turbulence of primary interest at Hvassahraun.

### 1.3 Turbulence Metrics

Atmospheric turbulence is three-dimensional and governed by non-linear relations, making it very difficult to describe or quantify in a deterministic simple manner. Hence turbulence is primarily modeled as stochastic processes with characteristics that describe its behavior in terms of statistical properties. The fact that this phenomenon is a function of space as well as time makes this even more complex. However, to compute the effect that turbulence has on an aircraft in flight its components must be represented as functions of time. For this purpose, certain assumptions must be made that enable this mathematical description to be expressed in the time domain. This is based on a description of the power density of the turbulent wind components and the intensity of these wind gusts that make an aircraft deviate from its intended flight profile. A parameter, i.e. the so-called Eddy Dissipation Rate (EDR), has been adopted as a measure of the turbulent field intensity for aviation purposes by international agreements; ICAO<sup>1</sup> and WMO-ICAO 2014<sup>2</sup>. EDR is defined as the cube-root of the eddy (energy) dissipation rate, which is the rate at which mechanical turbulence energy is dissipated into heat through viscosity in the smallest eddies. Eddy dissipation rate is defined in units of energy per kg per second  $((\text{m/s})^2/\text{s})$ . The EDR metric was originally suggested in 1964 and can be estimated from time series data of vertical wind or vertical aircraft acceleration based on acknowledged models expressing the spectral distribution of turbulence in the frequency domain. For a given aircraft (wing loading, change of lift due to angle of attack variations and true airspeed), RMS vertical acceleration is proportional to EDR. Aircraft "bumpiness" at a given EDR value will vary based on aircraft response to the atmospheric eddies. In general, increased wing loading (mass per wing area) reduces eddy effects on the aircraft, but increased speed has the opposite effect; hence, two dissimilar aircraft flying simultaneously through a turbulent atmosphere will not generate the same pilot report (PIREP) even if the pilots use the same rating scheme. Correlations between EDR estimates, RMS vertical acceleration measurements and PIREPs have been found to be very good. Thus, algorithms to estimate EDR have been implemented on several commercial air

---

<sup>1</sup> ICAO Doc 10045 MET 14

<sup>2</sup> WMO-ICAO, 2014: **Met divisional meeting—Initial draft roadmap for the World Area Forecast System (WAFS)**. WMO-ICAO Rep. MET/14-IP2 CAEM-15/INF.2 17/1/14, 16 pp

carriers with data automatically downlinked, effectively removing the pilot from the reporting loop. Turbulence and low-level wind shear forecasts and PIREPS are available to aviators for example in the US. This includes a chart to assist in evaluating the effect of EDR on airplanes in three weight categories.<sup>3</sup>

EDR will be utilized as the main turbulence metric in this report.

#### 1.4 Pilot Project of 2021

Easy access to instrumentation, instrument expertise and suitable airplanes provided an opportunity to try out various methods to build and test reliable and inexpensive measurement devices for measuring the vertical airplane acceleration coupled with GPS navigation for detailed 3D location information. A major challenge was how to isolate noise and mechanical vibrations from the turbulence-induced accelerations. The acceleration measurements, limited to a carefully selected frequency band, were used to calculate EDR. This turned out to correlate well with pilot assessment of the turbulence levels experienced by the test pilots. Based on this it was decided by the Ministry of Infrastructure to undertake in-flight measurements in the Hvassahraun area, alongside other traditional weather measurements accumulated at four height levels by a 30 m mast as well as a lidar unit stationed in the area. The process, instruments, the methods of data processing as well as some of the test results are described in a report dated at the end of 2021 in Icelandic titled: Mælingar á loftkviku yfir Hvassahrauni, Forverkefni janúar-september 2021<sup>4</sup>.

#### 1.5 Measurement Methods

For the measurements, a PX4 drone control unit is used to record GPS position at a frequency of 1 Hz as well as vertical acceleration at 200 Hz. The high sampling rate allows for digital filtering of the acceleration signal (a bandpass filter of 0.1-2 Hz) to get rid of unwanted noise and vibration. Post-processing yields an EDR value along the 3D flight track of the measurement aircraft.

#### 1.6 Aircraft Response to Turbulence

Light, moderate, severe, and extreme turbulence reported by pilots are aircraft-dependent. EDR on the other hand is a property of the flow field. A given value of EDR will for example cause little bumpiness in a high wing load aircraft or aircraft at slow airspeed but might make flying a light aircraft with low wing loading difficult or possibly unsafe. EDR of around 0.1-0.15 m<sup>2/3</sup>/s marks the onset of light turbulence (exceeding 1 m/s<sup>2</sup> average RMS acceleration) for most aircraft, whereas approximately 0.35 marks the start of severe turbulence for an ultra-light aircraft. A Boeing 737 at cruising speed will experience severe turbulence at an EDR value of 0.45. The book *Aviation Turbulence*<sup>5</sup> is an excellent source of information regarding turbulence and its effect on the flight of fixed-wing aircraft. The effect of EDR on different types of airplanes is addressed in more detail in Chapters 4 and 5.

---

<sup>3</sup> <https://aviationweather.gov/gfa/#turb>

<sup>4</sup> **In-flight measurements of air turbulence over Hvassahraun** - Pilot Project January-September 2021; RU Engineering Dept. Report Nov 2021.

<sup>5</sup> Sharman R. and Lane T. editors; **Aviation Turbulence**, Springer Publishing 2016

## 1.7 Typical Measurement Mission

The primary objective of the turbulence measurement program was to collect in-flight vertical acceleration data in an area deemed to be of primary importance for the siting of the airport in the Hvassabraun area and its vicinity. This was done by undertaking measurement missions which were planned to obtain reasonably dense spatial coverage in three dimensions of the area within a period of 1-2 hrs. during which stable wind conditions prevailed. The goal was to collect such measurements under varying meteorological conditions that would enable the development of a quantitative model that provided a good understanding of the nature of the turbulence conditions in the area. Each mission yields a snapshot of the turbulence status at the exact time and location of the aircraft. Connecting the snapshot with other measurements in the area may allow some generalization regarding the turbulence status overall. By performing such flights under varying wind conditions and correlating these to wind data collected continuously from fixed stations by accurate wind sensors it is possible to build statistical models that provide quantitative estimates of the statistics of the turbulence given the essential state of the environment. This is a challenging problem.

To explain further how a measurement mission is carried out and the type of data obtained, a typical flight flown on January 8th, 2022 is described. Three airplanes were used simultaneously for measurements flying at separate altitudes on that day.

### 1.7.1 Track and data presented in Google Earth

A Google Earth ground track (out of three on this date) is shown in Figure 1-1. A data analyst can follow each flight profile and read the essential measurement values enabling him to essentially experience the flight like a pilot and sense where high or low turbulence is experienced. The picture from Google Earth displays the track flown in green. The area of interest is marked by a red circle, which just touches the mountain ridge running NE-SW on the SE of the circle. The City of Reykjavik is visible NE of the area of interest. Also included at the bottom of the picture is the EDR (5s and 20s running averages). The red arrow marks the point of maximum EDR measured.

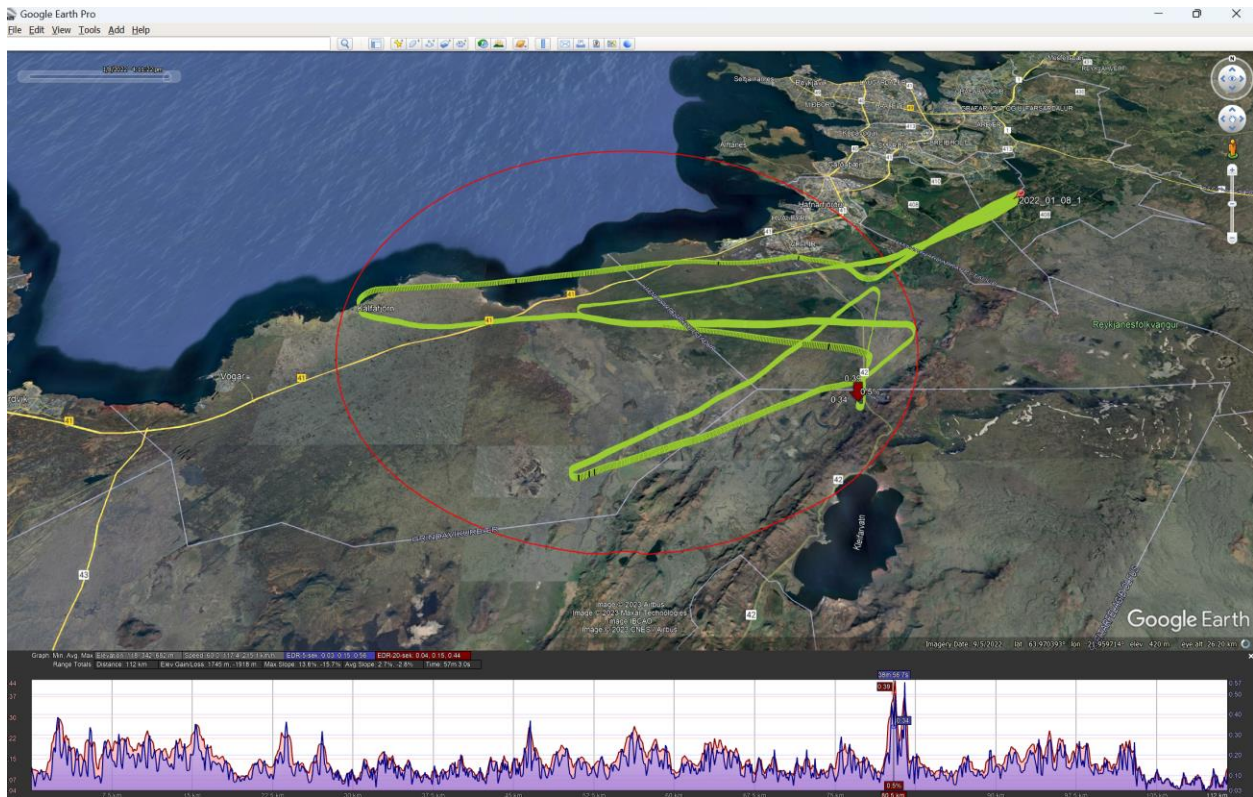


Figure 1-1 Flight track (green) on a Google Earth map provided for each measurement mission including a plot of EDR (panel on the bottom). The red circle marks the area of interest.

### 1.7.2 Quality Control of Recorded Measurement Data

Spectral analysis of the acceleration measurements is performed for each track to assure that frequency distribution is as expected, and that signal is not contaminated by acceleration “noise”. Also, the spectrum is plotted with the  $-5/3$  line in a log-log plot. If the data deviates significantly from the  $-5/3$  line, it suggests that the data is contaminated by noise or other related disturbances.

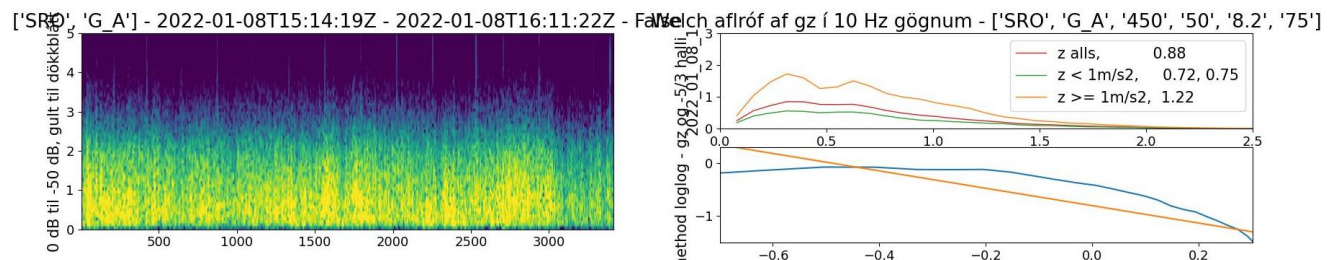


Figure 1-2 a) A spectrogram of power frequency with time. b) Power spectrum overall, and over or below  $1 \text{ m/s}^2$ . c) Spectrum with  $-5/3$  line. Data down-sampled to 10 Hz.

### 1.7.3 Measurement Data and EDR Contour Maps

An important aspect of quality control is comparison of the measurements with pilot experience. This measurement approach including instrumentation and processing has been tested in different aircraft and in various locations (well over 100 flight hours) with experienced pilots on board that subjectively evaluate the results. The track is plotted as acceleration time series and as EDR time series, and the pilots (PIREP) can look at the measured results to see if they match the experience during the flights in the way that pilot reports (PIREPS) are generated. Pilots have in general indicated that they agree with the measurements and never suspected that the measurements deviated much from their own experience during the flight.

Finally, the track is processed into a color code contour plot by interpolation between tracks within the area of interest. For more details see Appendix A: Visualization of In-flight Measurements. This yields visualization of EDR distribution for the area of interest.

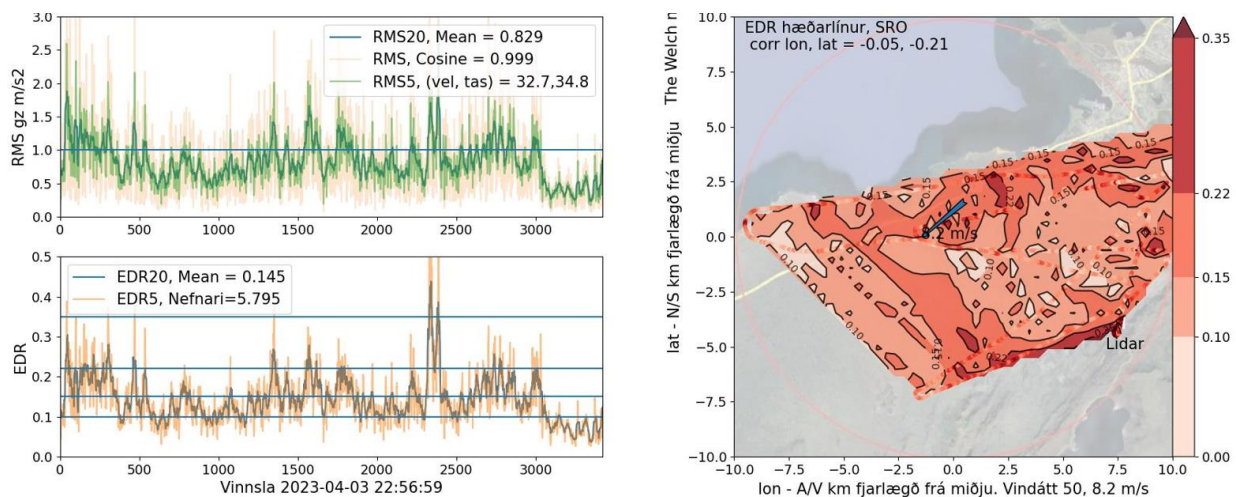


Figure 1-3 a) Acceleration measurements in  $m/s^2$  obtained at a rate of 200 Hz (filtered, 0.1 – 2 Hz, and rolling averaged to 1, 5 and 20 sec),  
b) EDR using rolling windows of 5 sec and 20 sec to compute average values.  
c) EDR contours for a single mission in the 20x20 km area.

EDR estimates obtained from acceleration data measured in-flight in the vicinity of the mast or the LIDAR is compared to EDR estimates obtained from ground measurements for consistency validation. The comparison and correlation of in-flight EDR data at various locations in the area with wind speed and direction obtained from the mast and lidar at fixed points are also essential for the building of models which may be used to assess the turbulence level at various locations.

Figure 1.4 provides EDR contour plots for a mission (Jan 8. 2022) involving three aircraft flying simultaneously at three different altitude levels. Each track has been analyzed and controlled for measurement data quality (see above), the tracks are joined, and through 3D interpolation a 3D data set of turbulence intensity in the volume explored by the measurement aircraft can be presented. Four horizontal slices at different heights are depicted in plots a), b), c) and d). Also, two vertical slices; East-West (E/W) in plot e) and North-South (N/S) in plot f). Both vertical planes include the mid-point of the area with the dark blue area showing the ground topography

intersected by these two planes. The multiple slices yield further understanding of the EDR distribution in the area.

Observations are for example that high EDR occurs over the ridge in the south-east, however this is not propagated towards the airport location but is carried downwind parallel to the ridge. In the middle of the area the lowest level (225 m) seems to have relatively high EDR which is probably generated by wind friction with the rough lava ground. This turbulence is not extending high up as is seen at the 475 and 600 m sections.

Clearly the 3D interpolation smooths the data, i.e. reduces the variability in the EDR values. A profile (track) run through the interpolated volume picking up the smoothed EDR values will demonstrate less variability than the original estimates derived from short-term acceleration measurements. This process is explained in more detail in Appendix A: Visualization of In-flight Measurements.

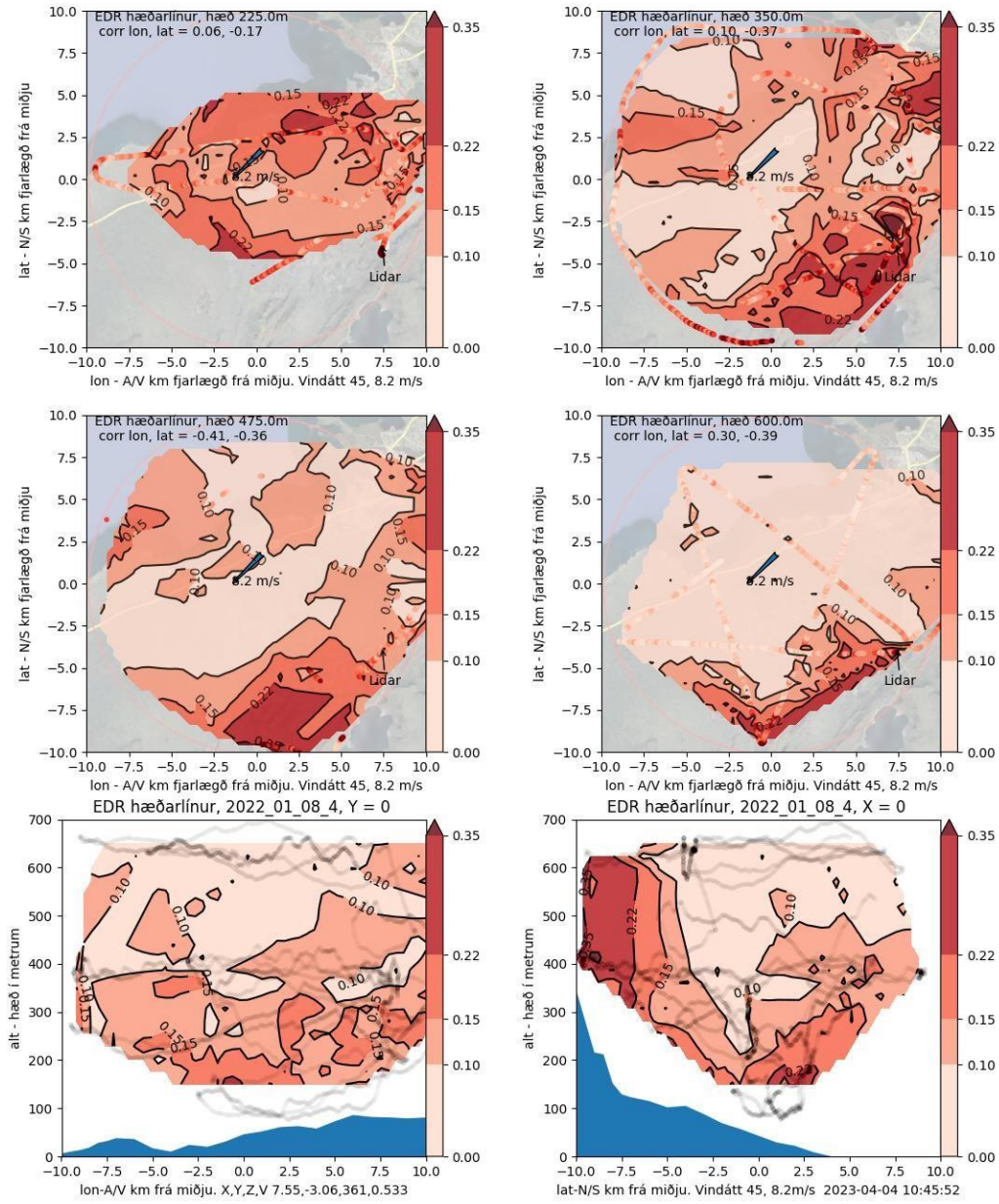


Figure 1-4 EDR Contour plots slices of the 3D interpolation field from mission of three aircraft. Horizontal a) 225 m; b) 350 m; c) 475 m and d) 600 m. Vertical East/West plane in plot e) and North/South plane in f).

## 2 Measurement Program at Hvassahraun Airport Site

### 2.1 Playing Area and Instrumentation

The idea of moving Reykjavik Airport (BIRK) to a different location in the vicinity of the city has been entertained and seriously considered for at least 70 years. The current evaluation of a location at Hvassahraun is focused on a point, 64.01 N, 22.11 W, assumed to be the “center” of the airport. Furthermore, it was decided that the turbulence area of interest would be within 10 km (~6 NM) of the center point which would contain most final approach profiles to runways. Therefore, these 314 square km become the area of primary interest for carrying out turbulence measurement. The weather mast is roughly 1.5 km west of the center point. A LIDAR system has been positioned intermittently close to the weather mast and for some six months at a site 8 km ESE of the center, in a quarry close to Sveifluháls.

Table 0--1 Important points locations

	Longitude	Latitude	Elevation (ASL)	Area of interest is a circle around Center
Center airfield	-22.11	64.01	28 m	Midpoint, R =10 km (6 NM)
Mast location	-22.140447	64.009322	28 m	R = 1 - 2 km
Lidar location, at quarry	-21.957887	63.976448	120 m	R = 1 - 2 km

EDR is estimated from ultrasonic wind speed measurements made in three dimensions and at four heights by the mast on a continuous basis as well as similar measurements made by the LIDAR along its measurement axis. These fixed-point measurements can be compared to EDR measured in flight close to these points. This yields an opportunity for relating continuous ground measurements to airborne (in-situ) measurements.

In the SE sector of the area, there are mountain ridges (350m ASL) running in the SW-NE direction. It is to be expected that on the lee side of these ridges a heightened level of turbulence will occur. This turbulence travels downwind as it dissipates and combines with other turbulence that originates from wind friction with the rough ground and possibly from thermal instability. In-situ measurements of turbulence (EDR) are expected to build an understanding of where and how turbulence occurs and how it is distributed at various heights in the measurement area.

### 2.2 Weather Conditions of Interest

The environmental conditions of primary interest are those when wind crosses over the mountain ridges; this occurs when wind is coming from directions of 80-210 degrees. Wind speed

approaching or exceeding 20 knots (10 m/s) is expected to generate significant lee side turbulence. If its magnitude and spatial distribution can be characterized through in-situ measurements the understanding of this phenomena will be greatly enhanced. Measurements during other conditions are also of interest as they generate further understanding of the wind/weather in the area and are useful to assess whether lee side turbulence is the dominant type of turbulence encountered in the area.

Weather forecasts have been matched with pilot/aircraft availability to initiate measurement missions when conditions are deemed of interest. Of course, turbulence in all weather conditions cannot be measured as these may not permit safe flight (visibility, precipitation, or excessive wind) or access to the area may have been restricted by air traffic control considerations. Hence, not all interesting wind situations could be measured. It was also decided to rely on light single-engine aircraft for carrying out the bulk of the measurements. This obviously has the advantage of low cost. However, it also provides a very responsive platform for collecting acceleration data at low and modest levels of turbulence due to a low wing loading and high bandwidth vis-a-vis turbulence frequency. Low cruising speed also results in longer time for data collection over a given distance, i.e. higher data resolution.

### 2.3 Measurement Methodology and Procedures

Pilots flying the measurement aircrafts were instructed to maintain constant airspeed, keep sharp turns to a minimum and maintain level horizon as much as possible and thereby minimize disturbances due to maneuvers on the vertical acceleration measurements due to turbulence. A mission typically generates a 200 km track, most of which is in Hvassahraun vicinity. Measurements are normally initiated before take-off and stopped after landing. Each track is processed after landing yielding EDR information along the flight profile (3D and time), and interpolations between tracks provide spatial estimates for EDR distribution. The results are mostly displayed as EDR surface contours in horizontal planes at fixed elevations in the Hvassahraun area. EDR contours on vertical planes are also provided, most of them containing the center point of the airport.

### 2.4 3D Presentation of EDR Measurements

Although EDR varies significantly over time at any given point in space, stable averages can be found. Measurements in the mast show significant fluctuation in time averages up to 10 minutes. These present significant challenges to consider when averaging data from flight measurements. Measurements in the air are done on “the fly”, where smaller aircraft typically fly at 40 m/s. Hence, a 10 minute average would correspond to averaging over a track of 24 km. Given the special nature of turbulence, this mixes not only time variance, but also the spatial variance. A 5 sec average along the track was chosen for most measurements which will then be representative of a reasonably small area (200 m track length), but of course this yields a very fluctuating EDR estimate because of the narrow time window. This window length represents a reasonable balance between spatial and time considerations.

Under the assumption that the time-averaged EDR field is relatively smooth and continuous, a linear interpolation scheme is used to calculate representative EDR values on a 3 D grid in the area of interest. The grid used was 50 cells by 50 cells for the area (20 km by 20 km) and 20 levels for 150 m to 650 m ASL. Results are presented (see also chapter 1.7.2) graphically by sectioning the interpolated 3-D field at various heights and vertical sections.

#### 2.4.1 Correlation of in-situ EDR Measurements with Met Mast

A multi-linear model is proposed to describe, in a more general sense than the contour plots, the EDR measured in flight within the area of interest (refer to section 2.1). It expresses EDR as a function of several spatial and meteorological variables: latitude, longitude, and altitude ( $x,y,z$ ) of the airplane, as well as with the 10 min average wind speed and wind direction at 30m elevation in the mast (mentioned in section 2.1), written as:

$$\widehat{EDR} = a \cdot D_{AV} + b \cdot D_{NS} + c \cdot H^2 + d \cdot H + e + f \cdot \bar{U} + g \cdot \bar{\theta} \quad (1)$$

The model coefficients were generated by least squares processing of relevant in-flight EDR data for both 5 second and 20 second measurements of in-flight EDR. The coefficients and statistical performance (level of correlation) of the model are shown in Appendix B, where the methodology is further explained. Based on this performance it was determined that the model shows great promise in expressing the general trend, i.e. the low frequency of EDR changes, but lacks the sharp peaks and valleys apparent in the measurement data. This can be seen by comparing Figs 2.1 and 2.2 below. When the 5 s and 20 s models are compared, they result in very similar coefficient values and trends. The 20 s model yields significantly better statistical (R-squared) performance results than the 5 s model as should be expected as the 20s data has smoothed out the sharpest peaks of the 5 s data. The authors believe that the model created in this way is a useful tool for representing EDR over the area.

One way of evaluating the quality of the correlation is to compare a real flight track with a simulated track. This is done by following a real flown track ( $x,y,z$  coordinates as a function of time) but instead of using the measured EDR value, the corresponding correlation model value is plotted. Plots are presented here to introduce this methodology, but more are shown in Chapter 4. Fig 2-1 and 2-2 show actual tracks and estimates (EDR vs. time, light green are 5 s results, dark green 20 s), in addition to the estimates provided by the correlation models on the same tracks plotted as solid lines. The plots are for positions within a 10 km radius from the assumed center of the airport. Gaps in the data appear where the measurement airplane leaves the area of interest.

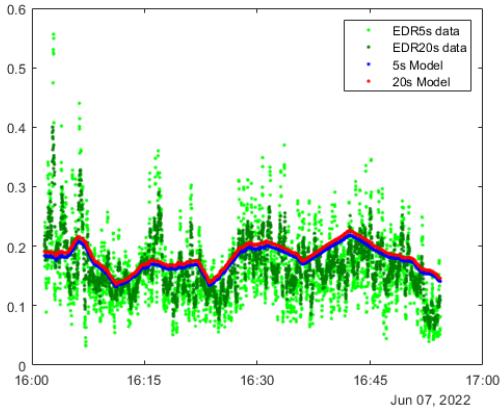


Figure 0--1

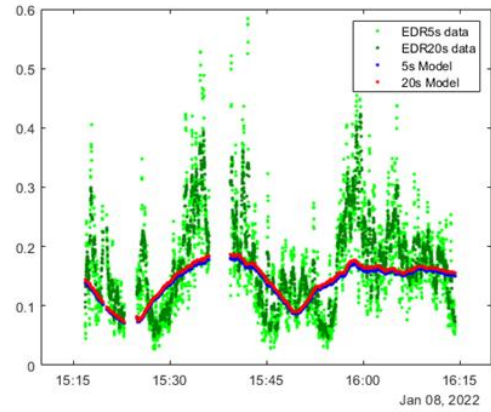


Figure 0--2

## 2.4.2 Correlation with Lidar Measurements

As mentioned before, a LIDAR was setup near the mast for a period of some months at the start of the measurement program. This was subsequently moved to a quarry near the mountain ridge some 8 km to SSW of the center point for the remainder of the in-flight measurement period. The intention was for the LIDAR to bridge the gap between mast measurements and in-flight measurements, and to quantify relations between ground measurements and in-flight measurements. However, due to technical difficulties, the LIDAR was not recording data continuously. As a result of these difficulties, there were only five flight missions that were carried out during LIDAR coverage, and only three of those flights provided sufficient LIDAR data for useful comparison. Despite this, an analysis was carried out to determine the LIDAR vertical profile in high ground wind speed and compare it with mast data and flight data. Several conclusions were drawn from the analysis which are described in more detail in “Appendix C; LIDAR vertical profiles”, and in Chapter 4.

LIDAR profiles compared with flight data are shown below, the mast EDR profile is included in the figures.

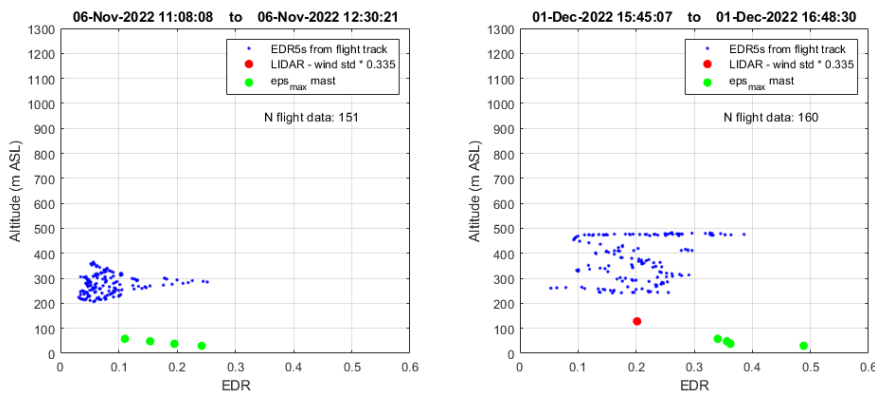


Figure 0--3 Flight Mission where LIDAR data was not available (except one point).

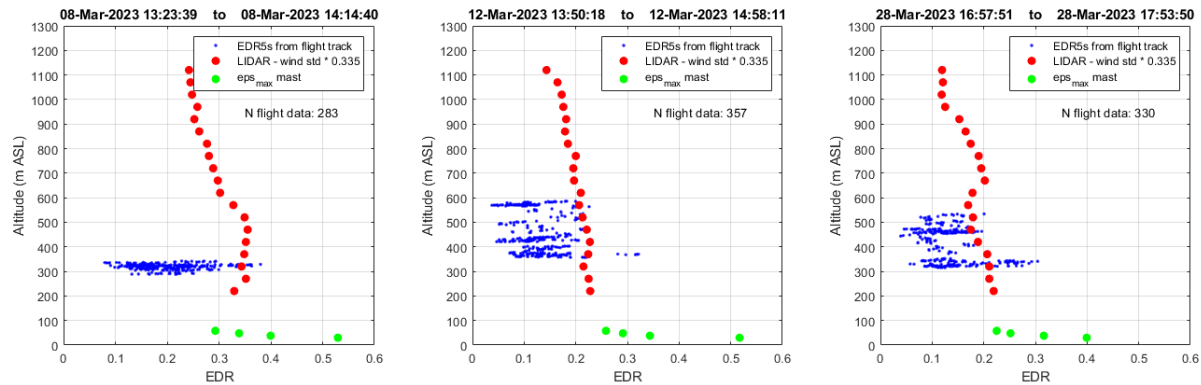


Figure 0-4 LIDAR profile with in-flight measurements of EDR and mast vertical profile drawn for three separate days over the quarry. Note that mast and LIDAR were not in the same location. The vertical profile is apparent, but the LIDAR results seem to be significantly higher than the apparent in-flight mean values observed.

### 2.4.3 Correlation with Belgingur Wind Forecast

Another attempt at relating the in-flight measurements with other sources of EDR data was done with the Belgingur (600m by 600m grid) meteorological forecast. Given the accuracy of the forecast for wind speed and wind direction, there was hope that the forecast could be used to predict the EDR over the area. Appendix D describes the process of evaluating the forecast for this purpose. The domain of the comparison was only a single point in the Belgingur forecasting grid, the exact location of the mast. Due to this fact, the analysis is not an overall evaluation of the Belgingur forecast and should not be used as such. It was only intended to determine if the forecast is useful for the application of predicting in-flight EDR.

The conclusions drawn are as follows: the forecast was most accurate for wind speed and direction 2 – 5 hours after the forecast update. Forecasting of wind speed and wind direction at the mast location was excellent and reliable. Forecasted EDR in the mast location and in-flight showed that the forecast captured the general trend but yielded significantly lower values than measured EDR. Furthermore, the forecast does not seem to capture the lee-side effect (or so the authors surmise) since the forecast more accurately predicts EDR values when the wind blew from the North. Some examples of in-flight data compared with the Belgingur forecast along with the model described in section 2.4.1 are shown below.

On each of the three measurement days the blue line (Belgingur EDR estimate along the track) is clearly much further away from the in-flight measurements along the track (green data) than the EDR estimates based on the data correlations, demonstrating that the forecast is underestimating EDR. From the conclusions drawn, the authors determined that the forecast should not be used to predict EDR in-flight or around the airport, at least in its current implementation.

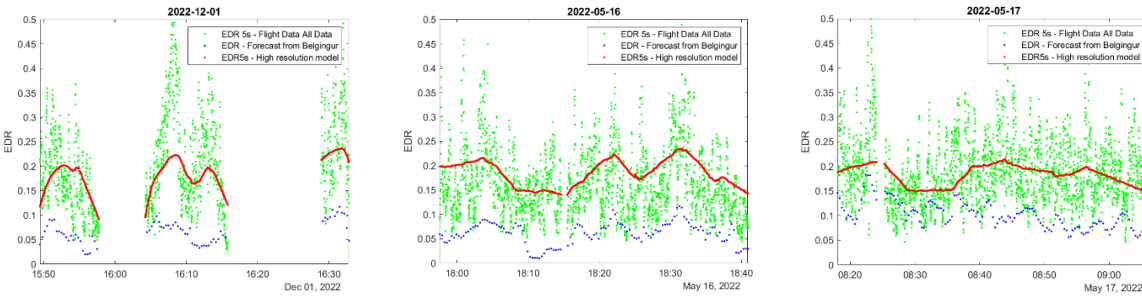


Figure 0--5 Three different measurement days; EDR 5s measurement (Green), EDR data through correlation model (Red), EDR forecast by Belgingur model (blue).

## 2.5 Network for Automated Collection and Processing of In-flight Measurement Data

Dedicated acceleration measurement equipment is the preferred method to make aircraft vertical acceleration measurements for the assessment of aircraft turbulence. However, acceleration measurements may also be performed by smartphones that are widely spread amongst the public. Smartphone measurements are of course less sophisticated than measurements with dedicated accelerometers and deliver less reliable results. A smartphone needs however not be installed in the aircraft like a dedicated sensor would be. Thereby, a long and costly authorization process is avoided. A MEMS (Micro Electronic Mechanical Systems) sensor for acceleration is built into most or all smartphones currently on the market. Additionally, smartphones are equipped with GNSS (Global Navigation Satellite System) receivers that are typically able to utilize satellites from the GPS, Galileo, Glonass and Beidou constellations. Furthermore, smartphones possess advanced data communications facilities in the form of 4G/5G mobile systems and Wi-Fi. Those features make smartphones ideal for setting up crowdsourcing of aircraft acceleration measurements by seeking cooperation with aircraft pilots or even with passengers. Using a smartphone in flight mode on board aircraft is not prohibited. In flight mode the smartphone can collect and filter acceleration data in real time and store it in memory. Aboard many aircraft, GNSS signal reception is possible, notably close to the windows and in the cockpit. Therefore, positioning and ground speed measurements are possible with a smartphone. This has been verified in many aircraft, e.g., Boeing 737, 757, 767, Airbus A321 and in De Havilland Canada DHC-8 (DASH-8). The data can be transmitted to a central server after landing when flight mode has been turned off. This can be done at any location where there is 4G/5G mobile or Wi-Fi connectivity.

There are drawbacks to this methodology. The smartphone needs to be placed on a horizontal surface onboard the aircraft which can be challenging, at least for passengers. A passenger doing turbulence measurements preferably needs to sit in a window seat and keep a nearly continuous attention on his/her phone so that it does not fall on the floor or is in a horizontal position. The speed measurement is ground speed and not airspeed as needed for the calculation of EDR. This error can be corrected though to a certain extent by finding the difference between the aircraft's

nominal cruising speed and the measured ground speed. Furthermore, weather information from the flown area can be collected and the airspeed assessed by postprocessing of the data.

Collection of data taken based on opportunity and by individual volunteers could be an attractive source of data on the general turbulence conditions experienced by the flying public in domestic as well as international air services. This could be important to identify where further measurement campaigns and studies could be of interest in order to better understand the nature and intensity of these disturbances to smooth flight and how they could potentially be avoided or mitigated.



### 3 Measurement Mission Reports

Measurements of air turbulence have been carried out and tested in various countries using aircraft of various types and categories. The first measurements in the Hvassahraun project were performed in 2019 using an Aaronia logger which at the time was a low-cost sensor that appeared to meet the requirements in terms of accuracy and cost. After several test missions these were found to be inadequate. The availability of drone controllers on the other hand seemed to offer a much more capable technical solution with an open public domain software environment for handling and processing the measurement data. After careful evaluation the inertial measurement sensor suite of the so-called PX4 controller, along with the associated GPS navigator, was selected for use in the project in 2021 at the initiation of the formal project period. Since then, measurements (with intention to compare to pilots rating, PIREPs) have been made on-board Boeing 757-200 in normal revenue operations (as passenger), Dash 8-200, ICP Ventura, Vans RV-9A, Ikarus C42 and several ICP Savannahs. It has never occurred that pilots have disagreed with or had any misgivings about the PX4 derived reports. Measurements have mostly been performed in Iceland, but also during cross-country trips in Germany, Spain and the US.

Results from Hvassahraun for different days were evaluated and grouped only after verifying a certain similarity in the results, i.e. a coherence in EDR evaluations throughout the measurement area. More details are found in Appendix E; Groups – Similar Conditions, and Chapter 4.

Some of the missions involved over-flying Reykjavik Airport, and Keflavik Airport on one occasion, on the way back from Hvassahraun to perform EDR measurements for comparison purposes. Results are given in Chapter 3.2 below.

#### 3.1 Aircraft Missions

About 75 missions, mostly by light aircraft, have been flown, each generating data in excess of 100 Mbytes, or a total of around 10 Gbytes. Many missions were flown to verify the measuring methodology and to validate post processing, partly by assessing pilot feedback from the measurement missions. 29 successful missions have been dedicated to the Hvassahraun area. Such a mission requires planning and preparation including instrument installation. For multi-airplane missions, pilots must be briefed, and plans must be made to ensure separation in a relatively tight area. Each mission requires around 2 hours of flying, of which 1-hour yields data directly of interest, typically generating a track of 125 km within the subject area. Several times up to three aircraft were successfully deployed at the same in the area. In these cases, tracks could be stratified, i.e. each aircraft was assigned a measurement altitude. For example, 500 ft AGL, 1200 ft ASL and 2000 ft ASL. Data was then combined in post-processing to yield a three-dimensional description of the EDR distribution in the area as can be seen for example in Figures 1.1-1.4.

Most missions originated at Hólmsheiði (ultra-light base) just east of Reykjavik, but the Dash 8 operated out of Reykjavik Airport. All flights were executed in good cooperation with air traffic control in the area although sometimes flight paths had to be adjusted to make way for other traffic. Icelandair supplied on two occasions a Dash 8 – 200 with crew to carry out measurements; on 6th Nov 2022, with wind direction of 60 degrees at 6 m/s and peak EDR20s 0.35 showing very similar results to what was obtained by 3 aircraft on 8 Jan 2022; and on 1. Dec 2022, wind direction 166 degrees at 11 m/s with peak measured EDR20s of 0.52. This resembles results obtained on 23 Aug 2021 with a Savannah aircraft. A more detailed description of the Dash 8 flights can be found in Appendix F; Dash\_8\_Missions.

Table 3-1 Overview of measurement flights

<b>Overview of the 29 measurement flights and registration of aircraft used</b>			
Including characteristic wind (direction and speed) in the 30 m Met Mast during flight			
TF-SRO, TF-205, TF-MET are all ICP Savannahs, TF-VTR is ICP Ventura			
TF-RVC is RV9A, TF-TXH is an Icelandair Dash8-200			
Date	degrees °	m/s	TF-
25.05.21	130	10	SRO
23.08.21	145	11	SRO
22.12.21	120	5	SRO
29.12.21	20	8	SRO, 205, MET
04.01.22	120	1	SRO, 205, MET
08.01.22	45	8	SRO, 205, MET
02.05.22	110	5	VTR
15.05.22	150	9	VTR
16.05.22	100	8	SRO, VTR, MET
17.05.22	90	7	SRO, VTR, MET
27.05.22	320	4	VTR, RVC
07.06.22	135	10	SRO
23.08.22	0	4	SRO
06.11.22	60	6	TXH
01.12.22	165	11	TXH
08.03.23	65	12	SRO
12.03.23	15	12	VTR
28.03.23	65	8	SRO

Below we show three typical mission reports which are used to evaluate and understand the EDR situation in Hvassahraun. First mission is by a Savannah, second by Ventura and the third by a Dash 8 aircraft. Content of each report was explained in Chapter one and Figure 1.3.

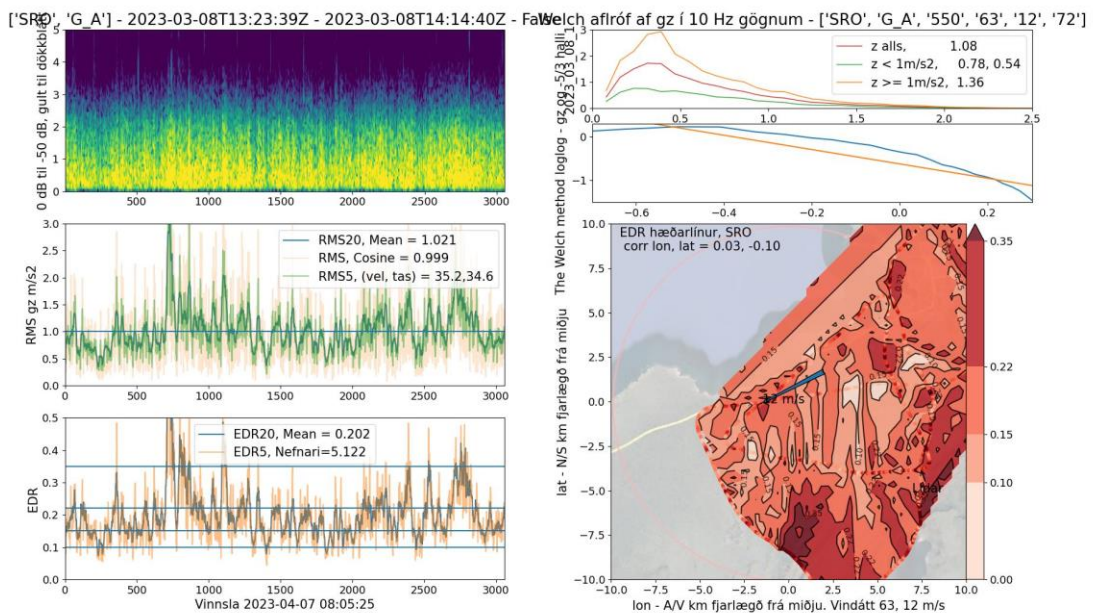


Figure 3- 1 Mini-report from 8. March 2023 for a mission with TF SRO and two pilots. Acceleration and EDR track are plotted as well as spectral information for acceleration. Finally, a contour map of the EDR distribution in the area. Pilots onboard confirm the contour map to be in agreement with their own experience. The highest EDR are in the vicinity of the hills in the SE.

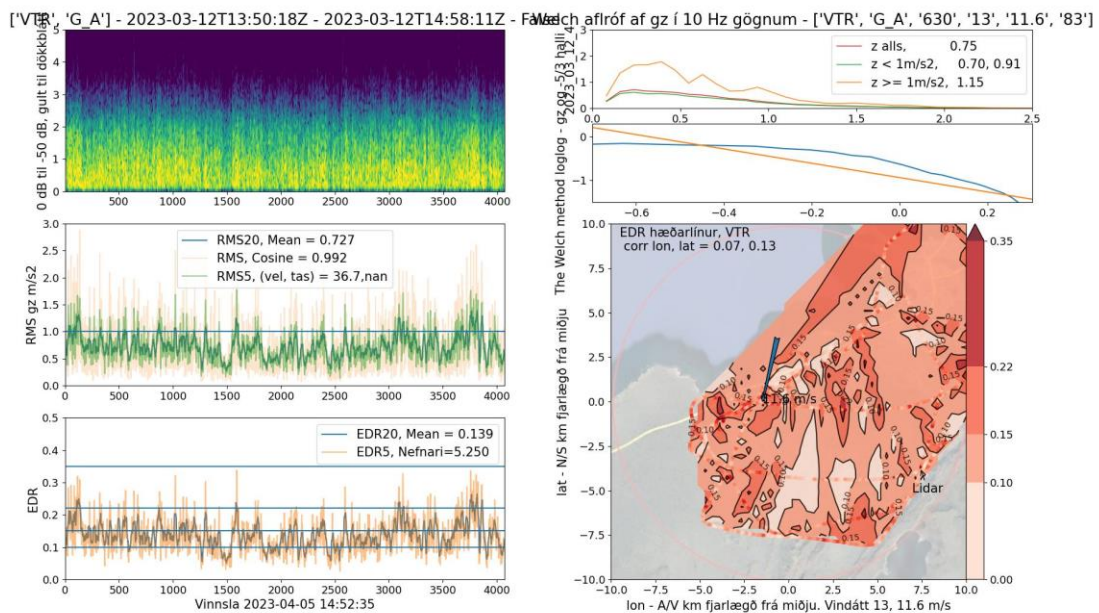


Figure 3-2 Mini-report from 12. March 2023, TF VTR and two pilots. With the northerly wind a high EDR towards the SE area is not observed.

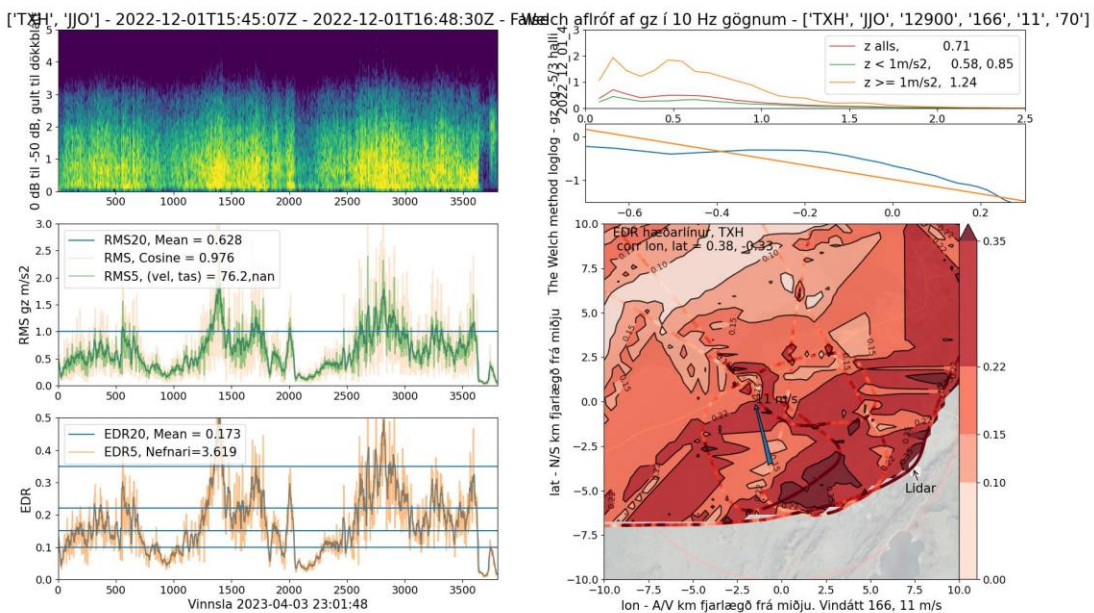


Figure 3-3 Mini report 1<sup>st</sup> of December 2022. The aircraft is a Dash 8-200 from Icelandair. EDR is highest towards the S and SE where the wind comes over the hills. The high EDR (like Fig 3-1) results in less aircraft RMS acceleration than evident by the smaller plane in Fig 3-1.

### 3.2 Comparison of BIRK and HVH

An important part of determining how intense the turbulence is over Hvasshraun is to compare it to other known and regularly flown locations. Several trips were flown over Hvasshraun and then directly over Reykjavik. In this comparison there were two points chosen to collect data, i.e. over the center of Reykjavik Airport and over the master Met mast in Hvasshraun (-22.140447 and 64.009322). The two points were chosen due to the high number of datapoints collected in the immediate vicinity. Datapoints within 1 km radius of each reference point and above 100m altitude were considered in the comparison. Each of the datapoints was then linked to a measurement of ten minutes mean wind direction and wind speed recorded by the top mast acoustic anemometers. Only data taken when wind speed exceeded 5m/s were used.

Figure 3-1 shows the results from the comparison. The points plotted are pairs of blue (over Reykjavik mid airport) and red (over Mast in Hvasshraun) that are mean values of EDR collected during the same flight. The vertical lines show one standard deviation of the EDR collected.

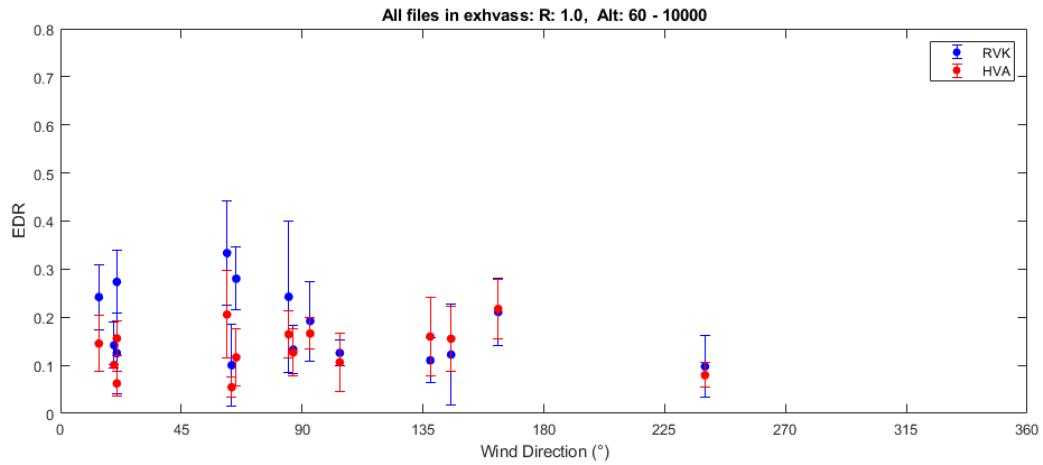


Figure 3-4 EDR- values taken close to reference points at BIRK (blue color) and HVH (red color)

The data suggests that EDR is lower over Hvassahraun in wind directions 0 – 110° but becomes higher from 110° onwards.



## 4 Turbulence Conditions in Hvassahraun

### 4.1 EDR Contour Plots of Measurements

Contour plots were introduced in Chapter 1, as well as the plots of sections in the 3D data interpolations used to enhance visual inspection of the results of measurements. The interpolation effectively smears out singular peaks in EDR, it works like a low pass filter, much like increased averaging time (1-5-20 sec) filters out individual peaks (in the 200Hz data) and delivers a smoothed average for display. The eye can spot trends in the contour plots, for example most plots show peaks in EDR over and on the lee side of the hills in S-E part, and a lowering value toward the sea in the N-W area. If the wind is easterly to southerly, the heightened EDR is carried by the wind towards the middle of the area. This is in line with what experienced pilots would have predicted. However, quantifying the difference would have been impossible without in situ measurements. Although all flights generate a contour plot, only a couple of examples are shown here (see also 3.1) while various wind direction and wind speeds are measured at the Weather Mast at 30 m height and marked on the plot. The contours are plotted for the specific height flown and listed in the plot title. In 4.3 below we show results of 3D interpolation from several simultaneous flights where variation with height can also be examined by plotting sections (contour plots) at certain heights in the 3D data.

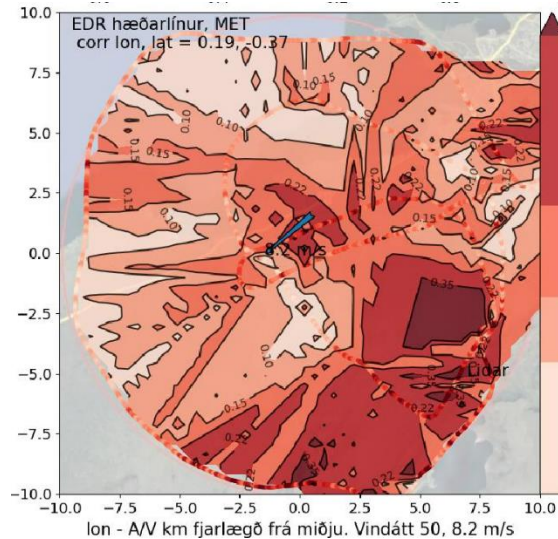


Figure 4-1 a) Jan 8<sup>th</sup> 2022 (400 m ASL)

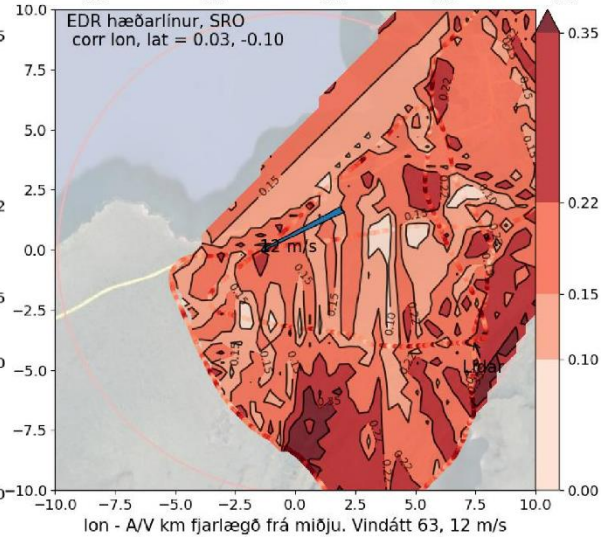
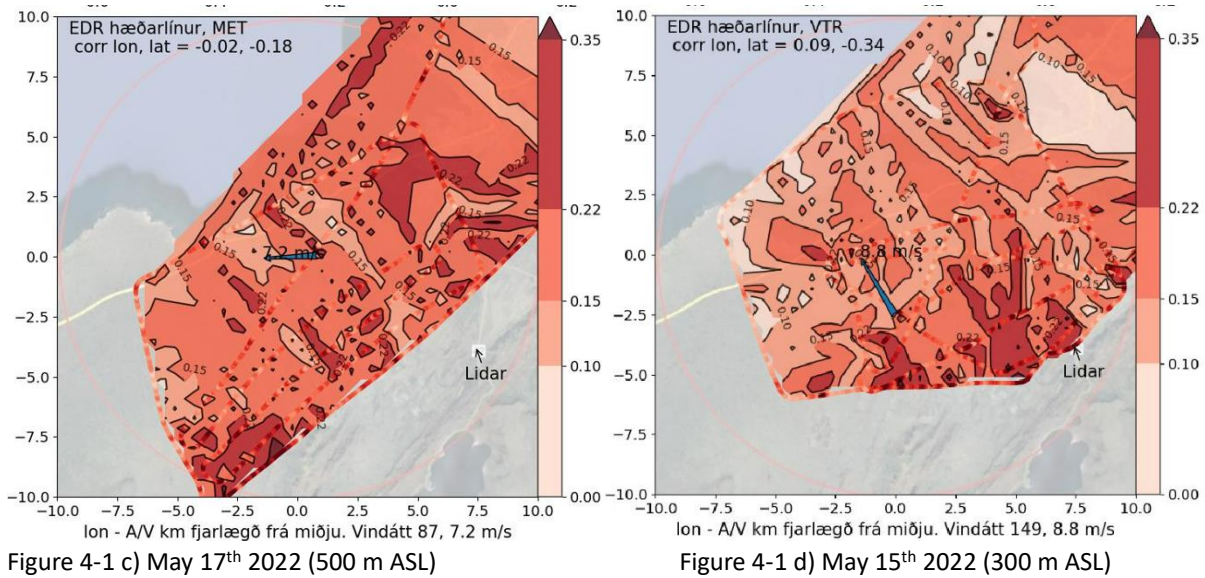


Figure 4-1 b) March 8<sup>th</sup> 2023 (300 m ASL)



## 4.2 Case studies of Flight Segments

During the first measurement flights in Hvassahraun it became evident that EDR was not evenly distributed in the area. Areas further away from the mountain range to the N-W and over the ocean, were always relatively quiet. As higher EDR values were of most interest the pilots tended to gravitate towards higher turbulence areas in the S-E area. A result of this is that average mission EDR values for full missions are meaningless for the mission area as a whole because of the flight track bias towards higher EDR subareas.

Typically a track will have peaks (gRMS20) that are 2-3 times the average RMS value for the whole track as shown in Appendix G; Statistics of Vertical Accelerations. For example, the average RMS value of  $3 \text{ m/s}^2$  may result in peak acceleration of  $1 \text{ g}$  ( $9.8 \text{ m/s}^2$ ) which is generally considered to be severe turbulence as an unrestrained object would lose contact with its base.

The highest gRMS20 measured in the area was  $2.8 \text{ m/s}^2$ , but the highest EDR value was just over  $0.5 \text{ m}^{2/3}/\text{s}$ . Of course, the values based on 5 s or 1 s rolling averages were much higher. However, the estimation error of these short-duration estimates is significantly higher than that of the gRMS20, given that several minutes are needed to estimate a “true” value. Pilots flying the missions described these peak situations as severe turbulence (i.e. momentarily out of control, loose things shift around etc.). One example of a track from the Ventura aircraft (Figure 4-2, May 15<sup>th</sup>, 2022), is included here showing a gRMS20 max of  $2.7 \text{ m/s}^2$ , and a gRMS5 of well over  $3 \text{ m/s}^2$ . This resulted in EDR20 of  $0.4 \text{ m}^{2/3}/\text{s}$ :

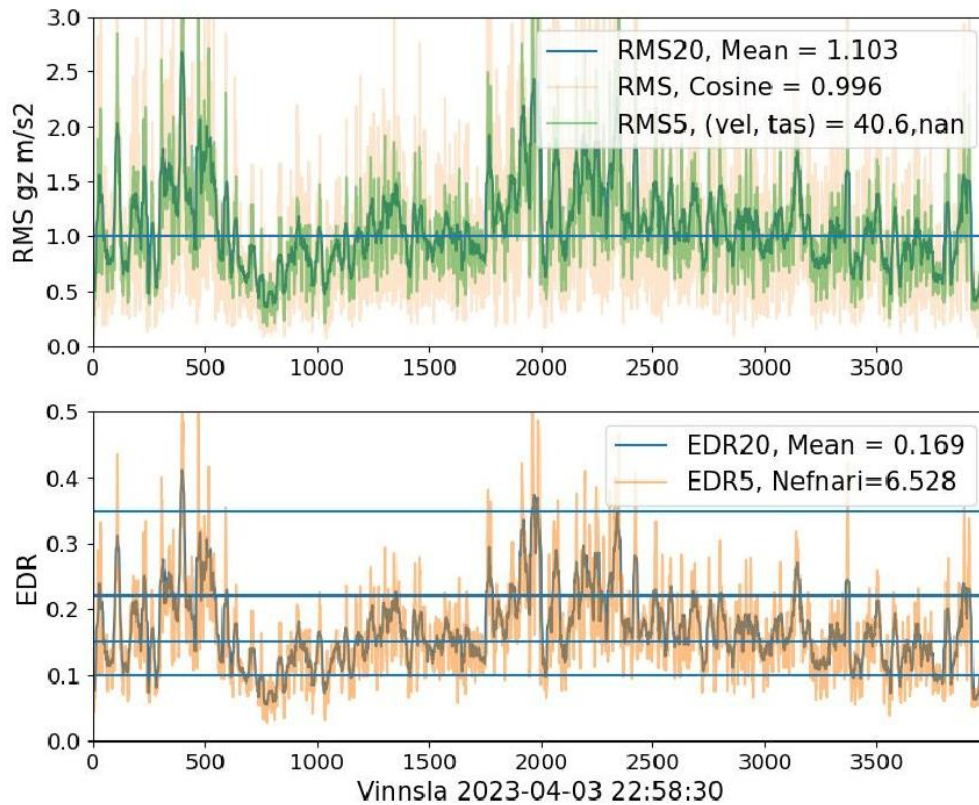


Figure 4-2 Showing acceleration and EDR graphs from one flight. As can be seen the mean EDR is 0.169

### 4.3 Grouping of flight segments under similar conditions

The Hvassahraun missions were grouped based on weather mast measurements, and corresponding data combined for visualization.

The first group for low wind (less than 5 m/s, thermal) conditions is best described by the following figures which are based on 6 flights. All the flight data is pooled and then 3D interpolated and drawn exactly like Fig.1-4 above. The level of turbulence is low but increases close to and above the hills in the south or east of the midpoint. Experienced glider pilots would confirm the expectation of turbulent activity from unstable thermals, often triggered by hills in the landscape, dry fields or sandy areas that are readily heated by sun radiation. The flight tracks (black) are visible in subpictures 5 and 6.

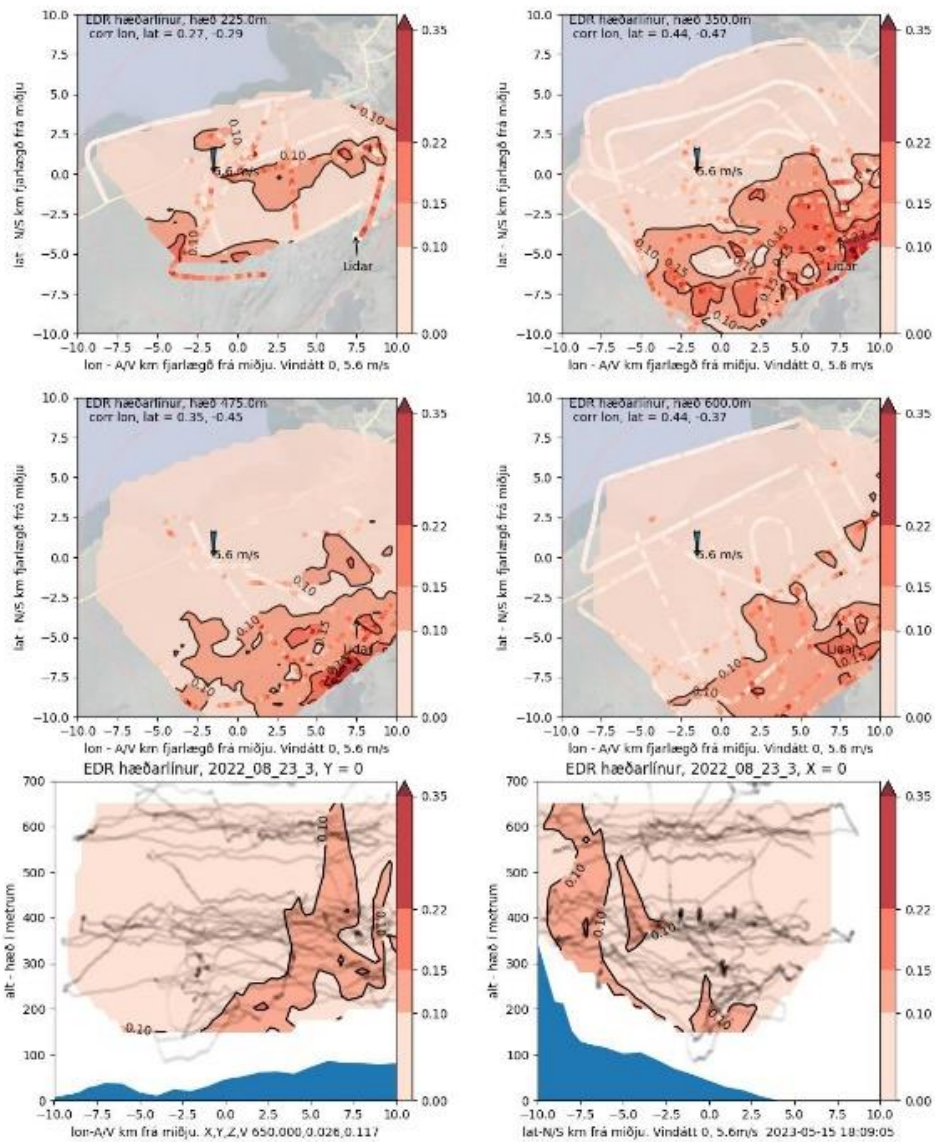


Figure 4-3 Shows the 3D interpolations of grouped flights and their cross sections. First 4 subfigures show horizontal cross sections at different heights. The bottom two subfigures show vertical cross sections east-west and north-south respectively.

For situations where wind exceeds ~5 m/s we group on the one side missions with wind direction from 0-80 degrees. The average direction is 40 degrees (~NE), and average wind speed 8.1 m/s from 11 flights. And on the other side missions with wind from 80-180 degrees. The average was 116 degrees (~SE), average wind speed 8.6 m/s from 12 flights. Plots are provided in Figures 4-4 and 4-5, for the weighted average direction and wind strength measured at mast at height of 30 m for the two separate wind directions.

The difference in EDR values is significant considering that the difference in average mast wind speed is only 6 %. Figure 4-5 (SE) shows EDR in every section 30-50 % higher (darker red color) than Figure 4-4 (NE). The higher EDR at the mountain top with SE wind extends downwind towards the airport location with EDR reaching local maximum at mountain peak height. The NE wind shows maximum EDR over the mountain top, whereas with SE wind this occurs immediately downwind on the lee side. A vertical plot of the NE wind EDR with height, at airport location would be expected to decline from bottom where the turbulence is generated. This is confirmed by subpictures 5 and 6. For SE wind the flow over mountain peaks contributes to the EDR intensity in addition to that generated by surface friction. This appears to generate a local maximum at roughly mountain peak height and is carried downwind towards the middle of the area. This is examined further in sections 4.4 and 4.5 below. The in-flight measurements appear to confirm the previously acquired qualitative estimates that turbulence is especially high in the area when wind is coming from directions 80-180 degrees.

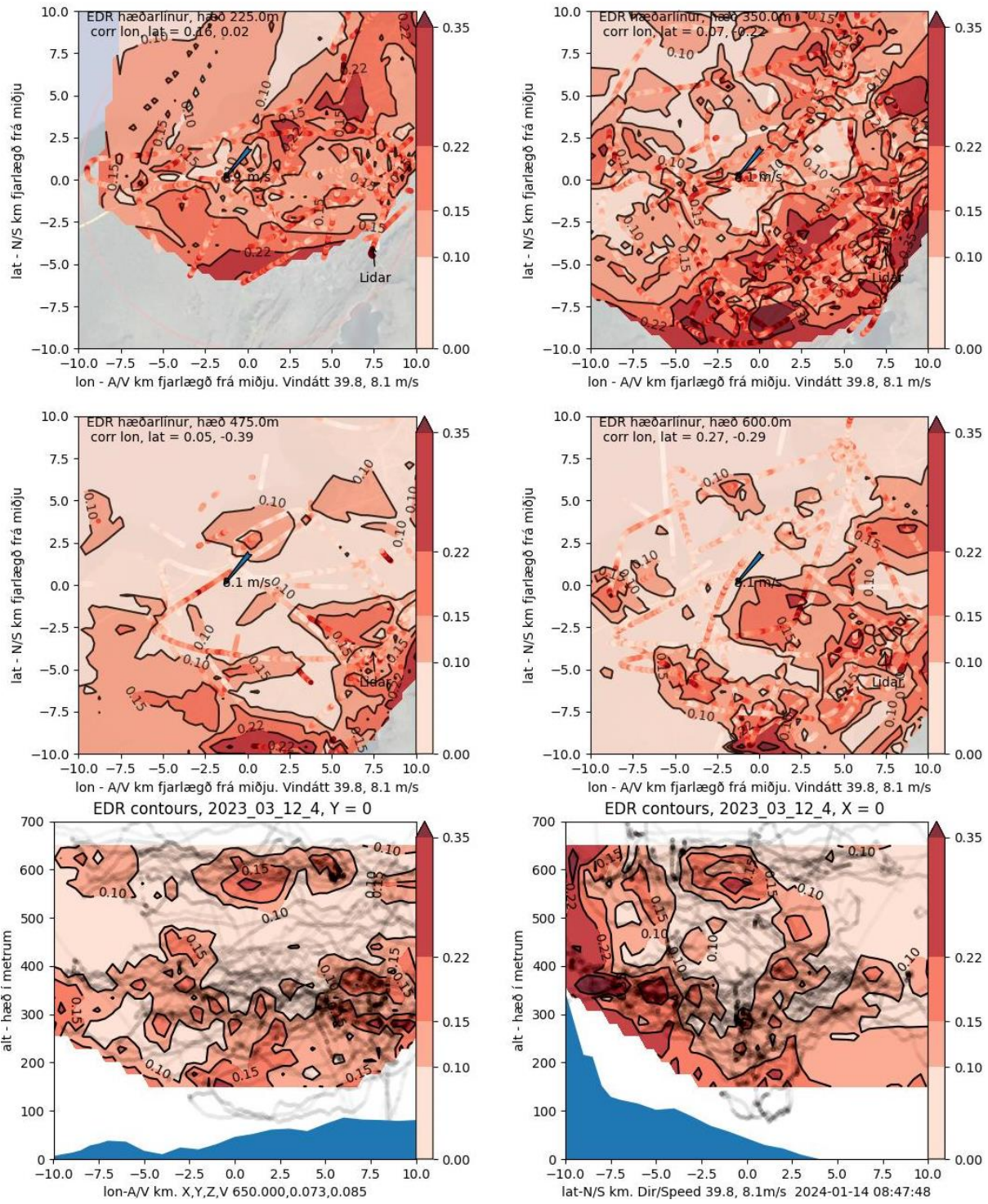


Figure 4-4 The 3D interpolations of grouped flights 0-80 degrees, and their cross sections. Average windspeed and direction is 8.1 m/s and 40 degrees. The first 4 subfigures show horizontal cross sections at different heights. The bottom two subfigures show vertical cross sections east-west and north-south respectively.

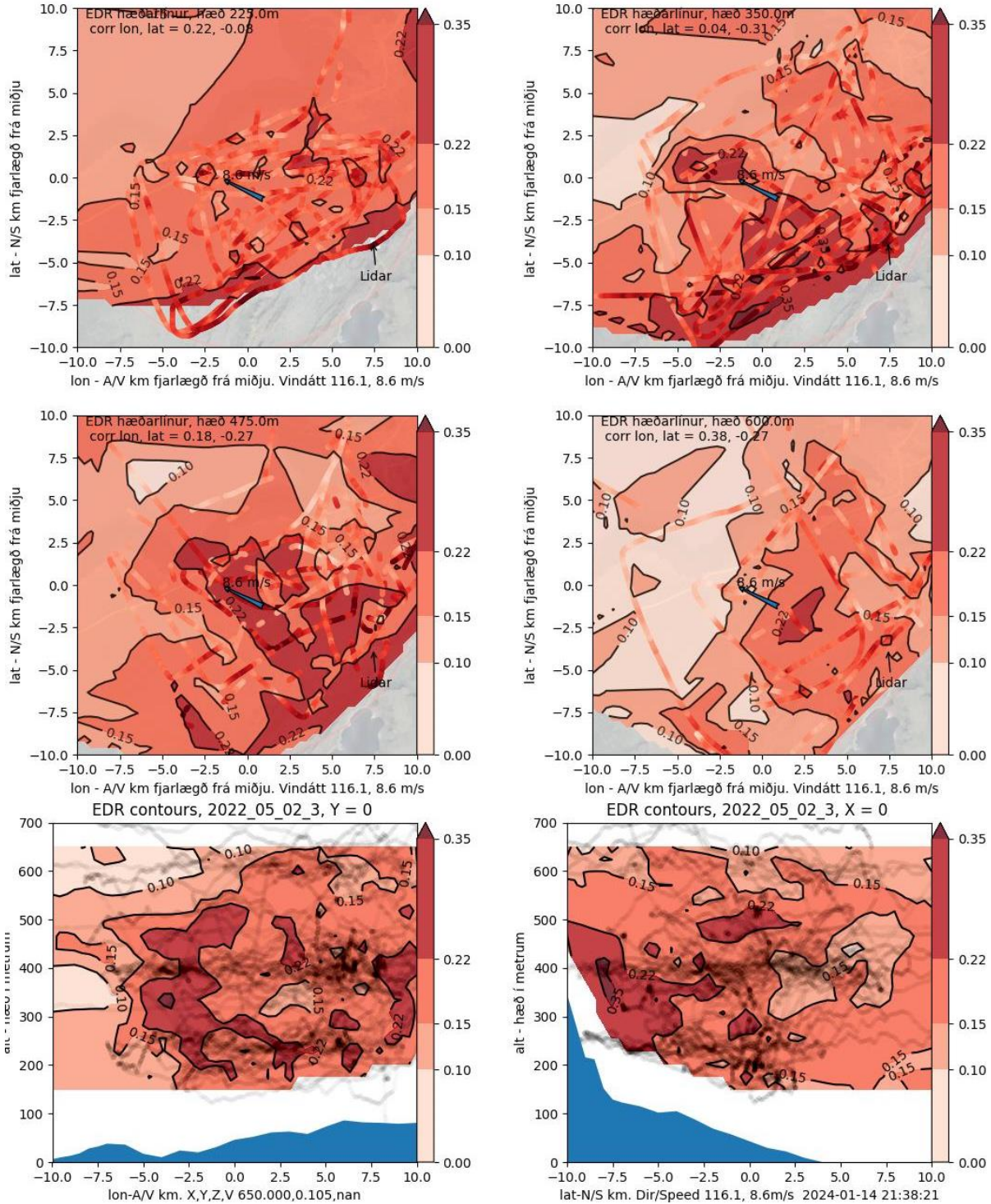


Figure 4-5 The 3D interpolations of grouped flights 80-180 degrees, and their cross sections. Average windspeed and direction is 8.6 m/s and 116 degrees. The first 4 subfigures show horizontal cross sections at different heights. The bottom two subfigures show vertical cross sections east-west and north-south respectively.

#### 4.4 Correlation of flight segments under similar conditions

In addition to the above graphical description of EDR results, a more quantitative approach using correlation models (Ch.2.4.1 above) can be used. Models were developed for three cases;

Case 1 = all flights (23) with wind above 5 m/s;

Case 2 = only flights when wind from 0-80 degrees (11 flights), see Figure 4-4;

Case 3 = for the wind sector of 80-180 degrees (12 flights), see Figure 4-5.

Root-mean-square-error (RMSE) and correlation coefficients for the models are given in appendix 6.2: *High Mast Resolution EDR model*. The Models can also be compared to individual measurements tracks. When a correlation model has been established, for example for the SE wind sector (Case 3), a previously flown measurement track (x,y,z location) can be followed in order to generate EDR estimates along the track, calculated using the model. These results are subsequently compared to the actual measurements obtained on this same track. The results from a few flights for Cases 2 and 3 are provided in the figures below. The model uses Mast (30 m, 10 minutes average) wind speed and direction at the actual time of the flight to generate results. Gaps in the graphs appear when the aircraft leaves the 10 km radius circle around the airfields assumed midpoint.

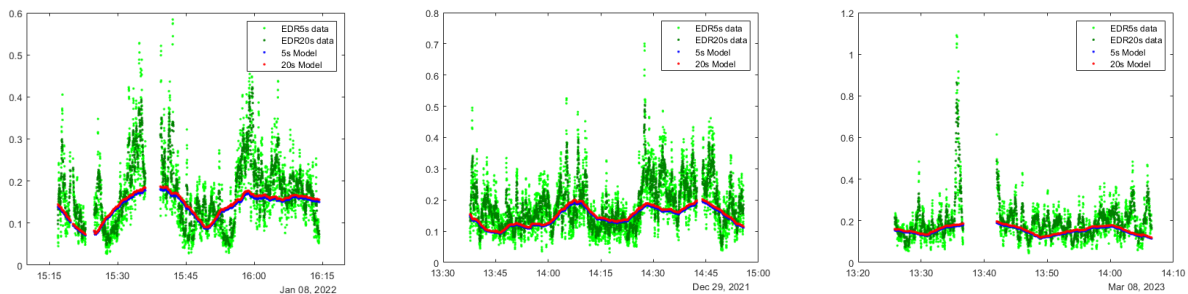


Figure 4-6 EDR from flights Jan 08 2022, Dec 29 2021 and May 08 2023. Comparing 5 s and 20 s rolling averages with Case 2 correlations models.

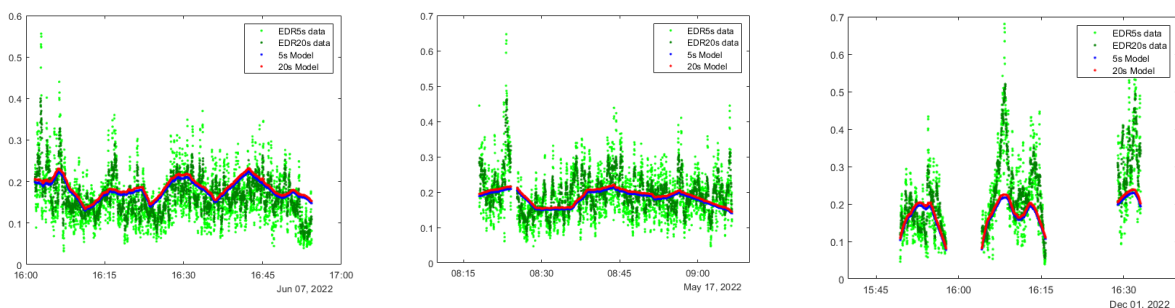


Figure 4-7 EDR from flights Jun 07 2022, May 17 2022 and Dec 01 2023. Comparing 5s and 20s rolling averages with Case 3 correlations models.

Overall, it can be concluded that using the correlation models appear to generate a realistic looking average track, although it is lacking in the higher frequency details. Especially, the peaks

and extremes that occur in “real” flights are missing. How to deal with this is discussed further in Chapters 4.8 and 4.9.

The curve-fits appear to track data better than the EDR forecast from Belgingur (a detailed analysis is provided in Appendix D; Forecast Comparison). Two flights that also include the forecast data from Belgingur for comparison to the Case 3 correlation model (see also Chapter 2.4.3):

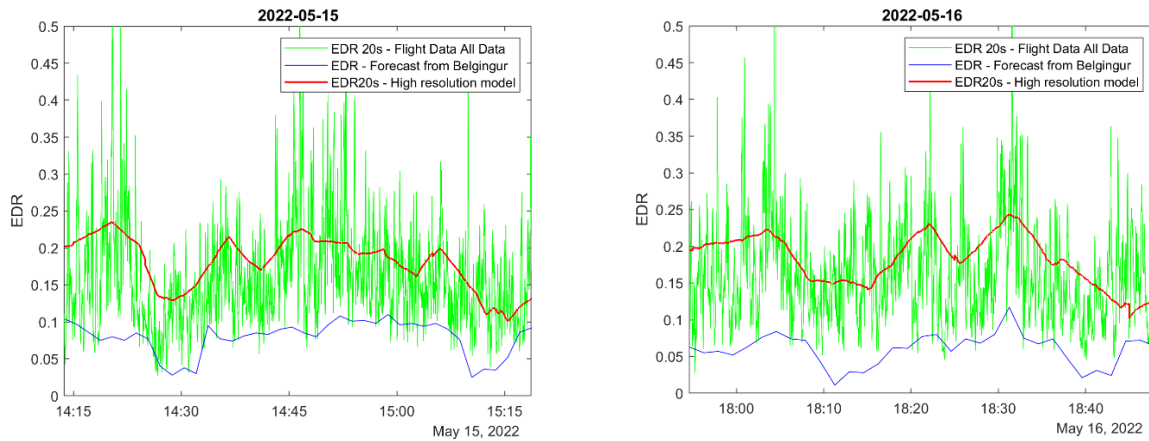


Figure 4-8 Comparison flight measurements with Case 3 correlations model and Belgingur forecast.

Individual flight tracks have been studied carefully but the authors believe that the compilations of data as done for Case 2 and Case 3 are more informative. The flight measurement data indicate that wind directions 80-180 cause, in general, higher EDR in the area than other wind directions. Hence, more effort has been spent on understanding and evaluating Case 3. Our results for Case 3 (see picture above) agree with what experienced pilots would predict, namely : Turbulence is highest on the lee-ward side of hill range; closest to the hills and drops off downwind from hills; and at hill top height. Intensity of turbulence increases with increased windspeed. It appears that the Case 3 correlation model captures all these essentials for a given wind-speed and direction at the 30 m mast. As our correlations are based on windspeed in the range of 5-12m/s, using them to estimate EDR for example at 25 m/s (see below) is an extrapolation that involves significantly higher uncertainty than interpolation.

Regardless, we can compute the Case 2 correlation model EDR data with mast wind at 25 m/s from NE (45 degrees) EDR based on 20 s running average for a point at (7 km, -7 km, 300 m) which yields  $0.24 \text{ m}^{2/3}/\text{s}$ . A 25 m/s mast wind from SE (135 degrees) on the other hand predicts  $0.35 \text{ m}^{2/3}/\text{s}$  from the Case 3 correlation model which is about 50% higher than for Case 2. Data from the Case 3 correlation model is provided for the whole area in the following figures for 25 m/s at 135 degrees. The figures are a contour plot done in the same way as fig 1.4 above. Instead of using measurements data for the picture we use the values given by the Case 3 model.

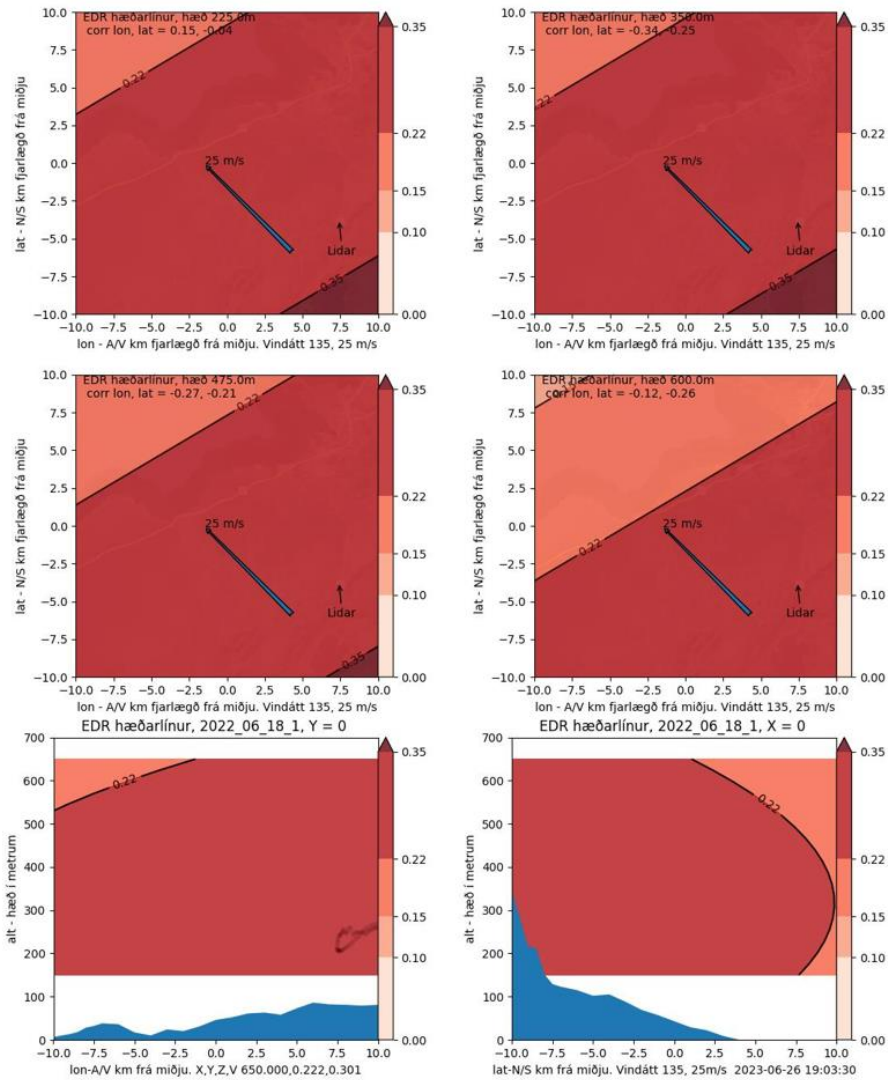


Figure 4-9 EDR Contour plots slices of the 3D interpolation field from Case 3 correlation.

#### 4.5 Comparison of Correlation Model and Independent Flight Results

The Icelandic Coast Guard (LHG) flew their Dash 8 several times through our area of interest May 16<sup>th</sup> 2023 during SE winds at around 12m/s. We were given access to their flight track data as well as acceleration measurements from their flight data management system, therefore EDR along their track could be estimated. The tracks are shown in the figure 4-10 below.

Case 3 correlation model “predicts” EDR value of 0.19 for the locations of the LHG tracks for 12m/s winds from direction 130 degrees. We were able to evaluate 21 tracks from LHG inside our circle of interest. EDR results ranged from 0.14-0.26. Overall average EDR is 0.206, which is reasonably close to the above EDR value of 0.19. This exercise has increased the confidence in the Case 3 model significantly. It should also be noted that during the LHG flight the 30 m Mast EDR value was around 0.3.

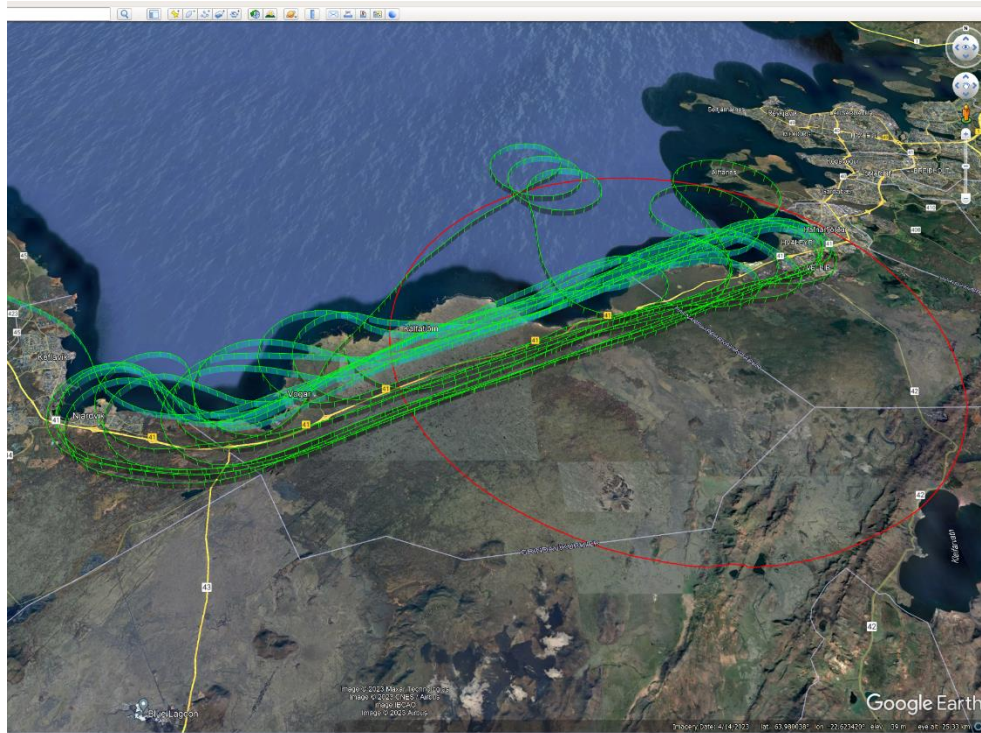


Figure 4-10 Tracks from the LHG Dash 8, May 16<sup>th</sup> 2023 and the circle of interest.

#### 4.6 Comparison of In-Flight and Mast Measurements

Another conclusion can be drawn from the correlations for Case 3 (80-180 degrees); From the above figure (4-5, EDR Contour plots from Case 3 correlation) we conclude that a point at (7 km, -7 km, 300 m) can represent the high EDR point for the area. If Mast EDR (at 30 m) is less than 0.25, then higher average EDR is found at our reference point according to the correlation. But if the EDR estimate in the mast exceeds 0.25, the correlation model yields a lower EDR in the SE area. For example, in relation to the above graph of the Case 3 correlation model, the Mast 30 m EDR is expected to be at 0.42 with 25 m/s wind from 135 degrees. This is demonstrated in the following graph which represents all in flight EDR measurements plotted against 10 min averages in the 30m mast. The added red points show the result of the correlation model for our reference point. If the correlation turns out to be representative for the EDR distribution even when winds exceed say 25 m/s, then the average EDR measured at the mast can be seen as the highest average EDR of interest in the area. Mast EDR can then be used to evaluate which airplanes should fly, and which ones not under the given wind conditions measured by the mast.

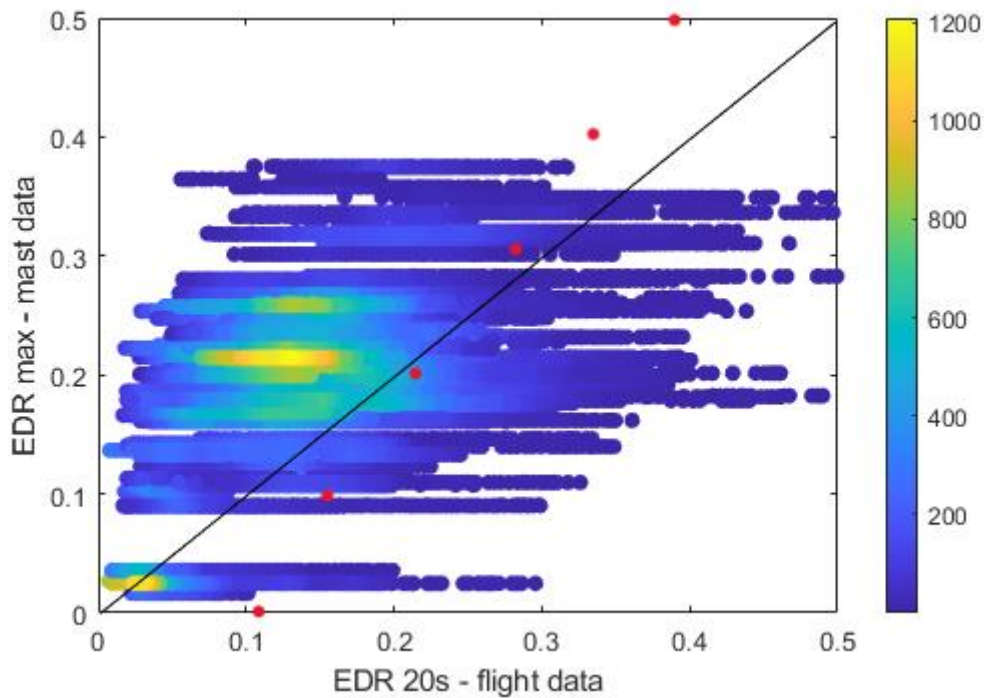


Figure 4-11 The color scale indicates the concentration of datapoints. The red points are Case 3 correlation results at (7 km, -7 km, 300 m).

#### 4.7 Comparison of in-Flight and Lidar Measurements

Comparison of flight data and LIDAR measurements can be used to validate the flight data and study the variation of EDR with height. Only 5 flight days were executed during which the Lidar was in service. Of these, only 4 days yielded data that could be compared directly to in-flight measurements. The data sets from these 5 days are shown in Chapter 2.4.2 above.

One advantage of the LIDAR is that it can deliver measurements when winds are too high for measurement flights to be performed. Below (Fig 4.12-4.15) are profiles segmented by the wind direction as dictated by the Mast. It reconfirms that the range of wind directions of primary interest (highest EDR) are 80-180 degrees. When wind speed at the Mast is higher than 12 m/s at the 30 m mast height we can evaluate data that could not be collected by our measurement

airplanes. Collecting these data sets yields the following distribution of LIDAR data over the Mast site with Mast EDR at all four heights included in the picture.

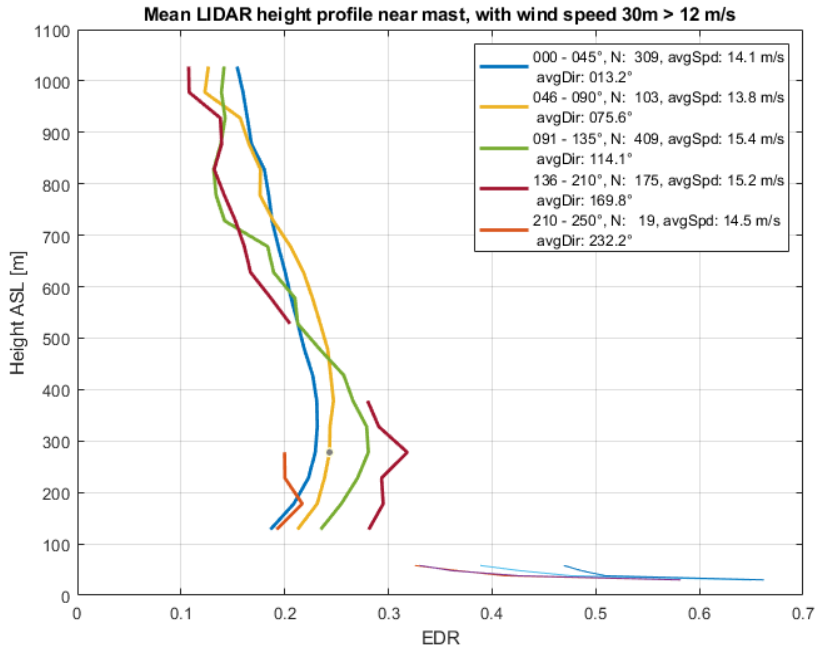


Figure 4-12 Mean LIDAR vertical profiles near the mast; wind speed at 30 m > 12 m/s. EDR in four heights in the mast are included.

Below is a compilation of all the Lidar measurements performed while the wind mast is indicating more than 12 m/s, segmented by wind direction. Also plotted are the results from the correlation model (based on the appropriate average wind speed and direction) for comparison. The agreement between the Lidar and the Model correlations are fair, and rather good for the wind directions over 90 degrees. This lends some validity to using the correlations beyond their strict validity, i.e. extrapolated.

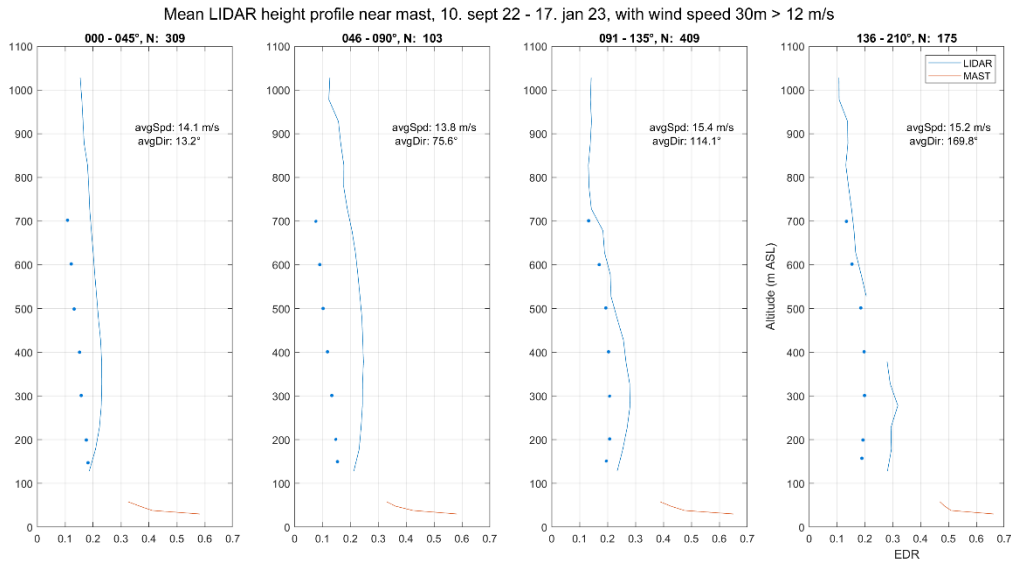


Figure 4-13: LIDAR vertical profiles with Case 2 (wind direction less than 90 degrees), and Case 3 correlations results (greater than 90 degrees)

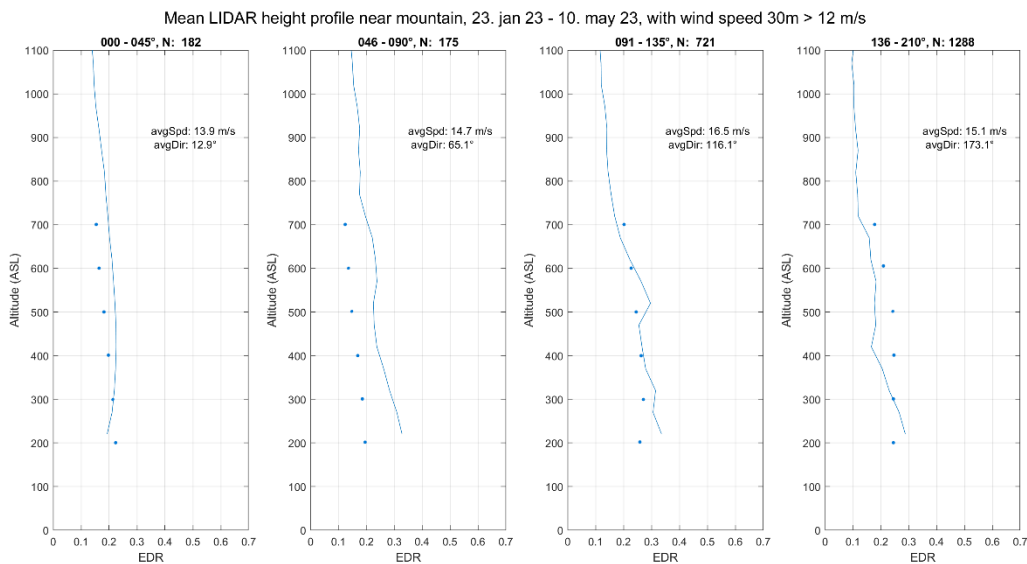


Figure 4-14: LIDAR vertical profiles with Case 2 (wind direction less than 90 degrees) and Case 3 correlations results (greater than 90 degrees)

#### 4.8 Overall assessment of Turbulence Conditions

The turbulence measurements obtained from the Mast, the Lidar and from in-flight acceleration measurements all demonstrate that turbulence (EDR) at any given location varies significantly with time. The most detailed and time-wise comprehensive measurements are obtained in the

mast. 10 minutes are needed to get stable (in time) averages. The same characteristic is evident from LIDAR. The flight measurements are averaged over 1 s, 5 s or 20 s, and display significant variability due to the short averaging time, but also due to the aircraft moving from one place to another bringing in spatial variability in addition to time variation. Appendix G addresses the statistics of vertical acceleration in-flight results and demonstrates for example that the 90<sup>th</sup> percentile value of in-flight measured EDR is roughly 1.6 times the average value regardless of the averaging time. Peak values can be more than triple the average values.

Examination of turbulence conditions that might prevent safe/comfortable flight in the Hvassahraun area is of primary interest. Based on the in-flight measurement campaigns (and other sources for Hvassahraun) this is expected to occur most often when the wind direction is 80-180 degrees, i.e. on the leeward side of the mountain ranges that surround the area. The report and pilot observations for Kapelluhraun (1970), about 5 km to the north of Hvassahraun, stated that with wind speed aloft exceeding 30 knots, landings, and take-offs there might be unsafe. The report is not very specific as to where the 30 knots are measured. If we assume that this is close to the ground (e.g. 10 m) this might be well represented by 20 m/s measured at the 30 m mast height. Looking at the correlation model for the area with wind at 30 m mast height of 20m/s and direction of 135 degrees, then at location (7 km, -7 km, 300 m) an average value for EDR (20s rolling average) can be expected to be 0.32. When this happens, EDR at the 30 m mast would be around 0.37. According to the statistical distribution of EDR this would imply that 10 % of the time the 20 s EDR would exceed 0.6 at that point. This level of turbulence is severe for small airplanes, but probably not for mid-size jets during landing or take-off.

#### 4.9 Criteria to mark severe Turbulence

The level of turbulence is determined from its effect on aircraft, i.e. the vertical aircraft acceleration at center of gravity. The acceleration can be described as RMS, or peak, over a certain time. ICAO<sup>6</sup> states that such peak acceleration between 0.5 and 1 g should be reported as moderate turbulence, and above 1 g should be reported as severe. In Aviation Turbulence data has been summarized, re-analyzed, and collected in the following table:

---

<sup>6</sup> ICAO Doc 4444, Procedures for Air Navigation Services — Air Traffic Management. ICAO PANS-ATM 2016. ISBN 978-92-9258-081-0

**Table 1.1** Turbulence reporting criteria and approximate atmospheric turbulence levels

Description	Aircraft-dependent measures			Atmospheric measures		
	Aircraft reaction <sup>a</sup>	Reaction inside aircraft <sup>a</sup>	Peak normal accel (g) <sup>b</sup>	RMS normal accel (g) <sup>c</sup>	$U_{de}$ (m s <sup>-1</sup> ) <sup>d</sup>	$\epsilon^{1/3}$ (m <sup>2/3</sup> s <sup>-1</sup> ) <sup>e</sup>
Light	Turbulence that momentarily causes slight, erratic changes in altitude and/or attitude (pitch, roll, yaw). or Turbulence that causes slight, rapid, and somewhat rhythmic bumpiness without appreciable changes in altitude or attitude (“chop”).	Occupants may feel a slight strain against seat belts or shoulder straps. Unsecured objects may be displaced slightly. Food service may be conducted and little or no difficulty is encountered in walking.	0.2–0.5	0.1–0.2	2.0–4.5	0.1–0.39 (0.1–0.21)
Moderate	Turbulence that is similar to light turbulence but of greater intensity. Changes in altitude and/or attitude occur but the aircraft remains in positive control at all times. It usually causes variations in indicated airspeed. or Turbulence that is similar to light chop but of greater intensity. It causes rapid bumps or jolts without appreciable changes in aircraft altitude or attitude.	Occupants feel definite strains against seat belts or shoulder straps. Unsecured objects are dislodged. Food service and walking are difficult.	0.5–1.0	0.2–0.3	4.5–9.0	0.40–0.69 (0.22–0.47)
Severe	Turbulence that causes large, abrupt changes in altitude and/or attitude. It usually causes large variations in indicated airspeed. Aircraft may be momentarily out of control.	Occupants are forced violently against seat belts or shoulder straps. Unsecured objects are tossed about. Food Service and walking are impossible.	1.0–2.0	0.3–0.6	≥9.0	≥0.70 (≥0.48)
Extreme	Turbulence in which the aircraft is violently tossed about and is practically impossible to control. It may cause structural damage.	Not defined	≥2.0	≥0.6		

<sup>a</sup>FAA (2014), Table 7-1-10<sup>b</sup>E.g., Lee et al. (1984), Lester (1993), Fig. 1-8<sup>c</sup>Bowles et al. (2009) based on running 5-s window<sup>d</sup>Gill (2014)<sup>e</sup>Peak over 1 min. ICAO (2013) definitions, updated values by Sharman et al. (2014) in parentheses

7

Figure 4-15 From the book Aviation Turbulence showing how the stages “light”, “moderate”, “severe” and “extreme” turbulence link to acceleration. Then the values of EDR are shown as an indicator for a large cruising aircraft.

Clearly, if the ratio between RMS and peak vertical acceleration is close to 3 then the two aircraft-dependent measures in the table are equivalent. Our own data (see Appendix G: Statistics of vertical acceleration) indicates this ratio, dependent upon time window, to be 2.3 (5 s) – 4 (60 s). This is further supported by Bowles et al<sup>7</sup>, figure 4-16, based on a 5 s rolling window. They state that the RMS acceleration value could be used as surrogate for the peak value. Further they showed that peak acceleration is proportional (i.e. multiplied by x 2.6) to the 5 sec RMS acceleration.

Sharman et al (2014)<sup>8</sup> correlated PIREP with measured EDR and came up with a simple quadratic fit. They concluded for a medium-sized aircraft (B757-200) in cruise, that average EDR of 0.47 would be reported as severe turbulence by the crew. However, this is the median of the EDR range with half of the PIREP reports falling between 0.12 to 0.72. They suggest that ICAO should revise their severe reference value for medium sized cruising jet to EDR of 0.48.

<sup>7</sup> R.L. Bowles and B.K. Buck; **A Methodology for Determining Statistical Performance Compliance for Airborne Doppler Radar with Forward-Looking Turbulence Detection Capability**, NASA/CR-2009-216769, June 2009.

<sup>8</sup> R.D. Sharman, L.B. Cornman, G. Meymaris and J. Pearson, **Description and Derived Climatologies of Automated in Situ Eddy-Dissipation-Rate Reports of Atmospheric Turbulence**, Journal of Applied Meteorology and Climatology, January 2014

The EDR values in the table have been updated even further by ICAO<sup>9</sup> such that severe EDR peak is now 0.45 (instead of 0.47).

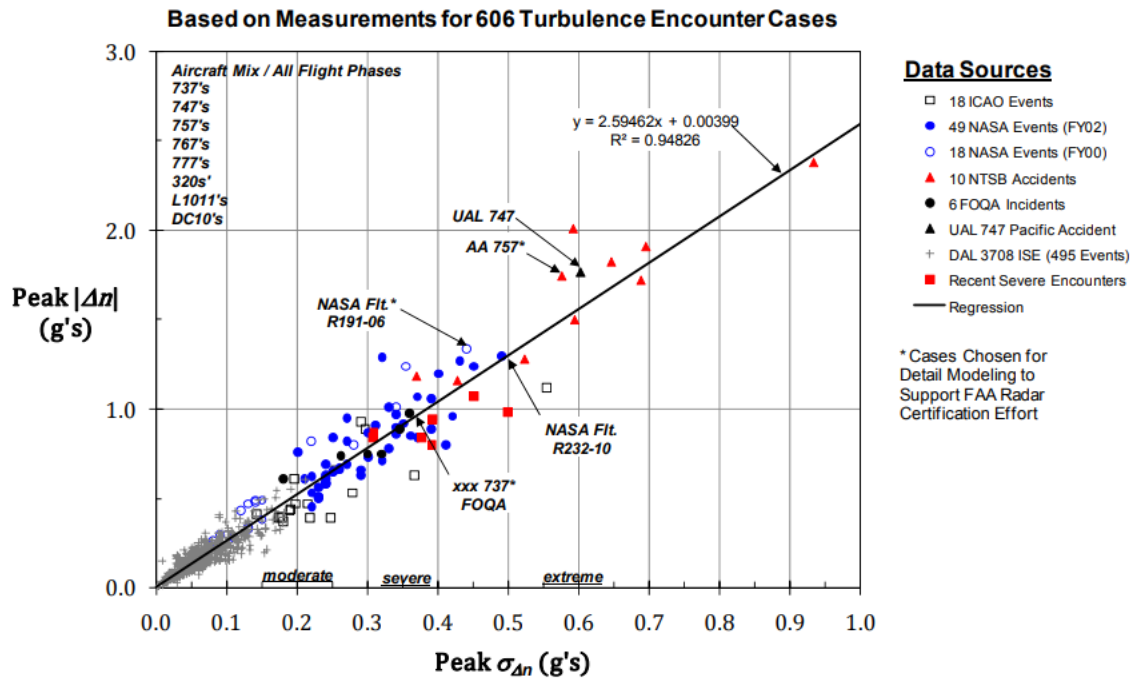


Figure 2: Correlation between Peak Load and Peak  $\sigma_{\Delta n}$  (5 sec. window)

Figure 4-16. Bowles et al (2009- NASA/CR-2009-215769).

Recent accident data (National Transportation Safety Report) based on 111 turbulence related air-carrier accidents (2009-2018) suggests that most turbulence related accidents happen in cruise and descent to flight attendants without seat belts fastened. The plunge model suggests that EDR of 0.45 for a cruising jet causes at center of gravity only  $1.3 \text{ m/s}^2$  RMS acceleration or roughly  $4 \text{ m/s}^2$  peak which may cause harm to unsecured people in an aircraft. We conclude that the large EDR spread of the PIREP reporting severe conditions for the B-757 ( $0.12$  to  $0.72 \text{ m}^{2/3}\text{s}^{-1}$ ) have led to the conservative reference value of 0.48 (now 0.45) and may not necessarily represent the ICAO\_Doc 4444 criteria. The EDR value of 0.45 is not in line with the acceleration values ( $0.3 \text{ g}$  RMS or  $1 \text{ g}$  peak, in figure 4-15) required to define severe turbulence, but is probably a good conservative value considering the spread around the estimate, chosen to reduce the likelihood of injury to unrestrained people on board. If people on board have seat belts fastened and all trolleys are stowed, a  $0.3 \text{ g}$  RMS acceleration is probably an appropriate mark for severe turbulence.

<sup>9</sup> ICAO METPWGMOG/7/SN/35 23/3/18

An aircraft acceptable EDR for approaching and departing aircraft has not yet been defined but has been called for. The ICAO<sup>10</sup> states regarding EDR: “...thresholds will only be applicable to “typical en-route conditions”, thus leaving the EDR metric for turbulence reporting undefined for approach and take-off.”

It is concluded here that the RMS derived vertical acceleration value of 3 m/s<sup>2</sup> is appropriate for marking the lower boundary of severe turbulence in a situation where all cabin persons are strapped in, and all trollies and baggage is stowed as is the case with departing or landing. This is the value that will be referred to when defining the turbulence limits set for operations from Hvasshraun. This value will be used to determine estimated EDR reference values that can be used to establish operational limits for different categories of aircraft.

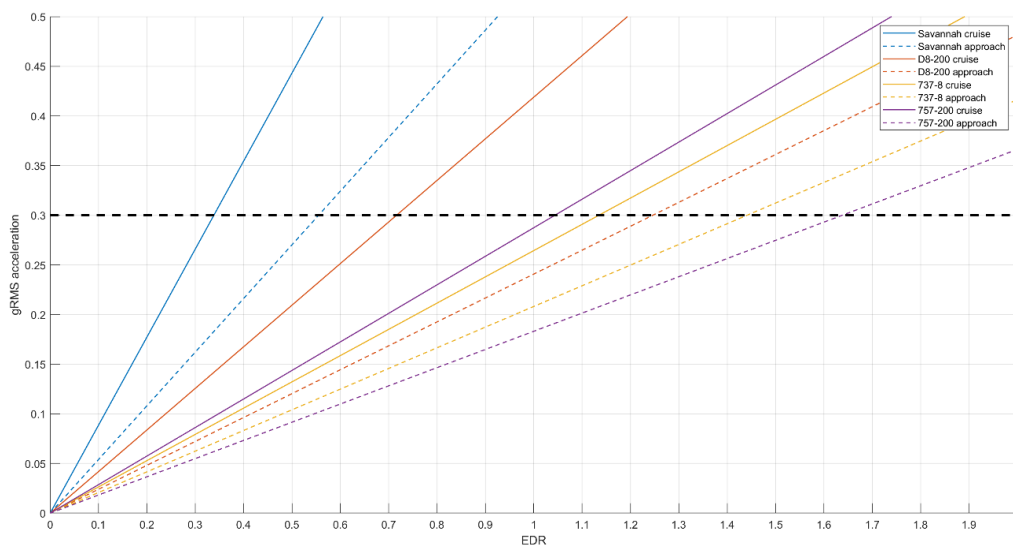


Figure 4-17. Four aircraft types in cruising and landing configuration, and their estimated RMS acceleration, specified in terms of g levels, for different EDR values. The criteria of 3 m/s<sup>2</sup> is marked on the picture as 0.3 g.

A plunge model is used to compute the relationship shown in Fig 4-17 for four types of aircraft, i.e. the Savannah ultralight, the Bombardier D8-200, Boeing 737-8 and B 757-200. Each aircraft type has a set of two lines in the same color, one solid line for aircraft in cruising configuration and a dashed line for aircraft in approach phase of flight. The horizontal line at 0.3 g marks severe turbulence according to the table above. 0.1 and 0.2 g would mark the onset of light and moderate turbulence.

If we take the EDR mark of 0.45 as entry into the severe turbulence regime for a mid-sized jet in cruise the same acceleration level for this category of aircraft in the landing mode is close to EDR 0.65-0.75. These values could be used to evaluate utilization limitations for an airport. We

<sup>10</sup> ICAO note CNS/MET SG/10 – WP/36 2006

still point out that if the  $3 \text{ m/s}^2$  criteria are used then EDR values well above 1 can be tolerated by midsize aircraft operating in the airport area.

Smaller aircraft might have difficulty operating when EDR is 0.4 or more. However, this happens at wind-speeds (according to our model) approaching or exceeding stall speeds of this type of aircraft or speeds preventing safe ground handling of the aircraft. It is therefore likely that the operation of such aircraft will be hampered more by the wind speed on the ground rather than the turbulence represented by EDR. As both factors are normally contemporaneous this would aggravate the situation.

#### 4.10 Anatomy of a severe turbulent event

The Savannah TF-SRO was flown from Rif (west Iceland) to Heiði (ultralight airfield) during strong northerly winds ( $20 \text{ m/s}$  at mountain top height). The flight involved flying close and low on the lee side of a  $1000 \text{ m}$  mountain with steep sides (Esja) during which severe turbulence was experienced. See the flight track, note that the coordinates of the color graph are defined in km from the midpoint of Hvassahraun airport. Peak accelerations appear at time  $3042 \text{ s}$  and  $3080 \text{ s}$ , well remembered by the pilot who confirms the events as severe turbulence.

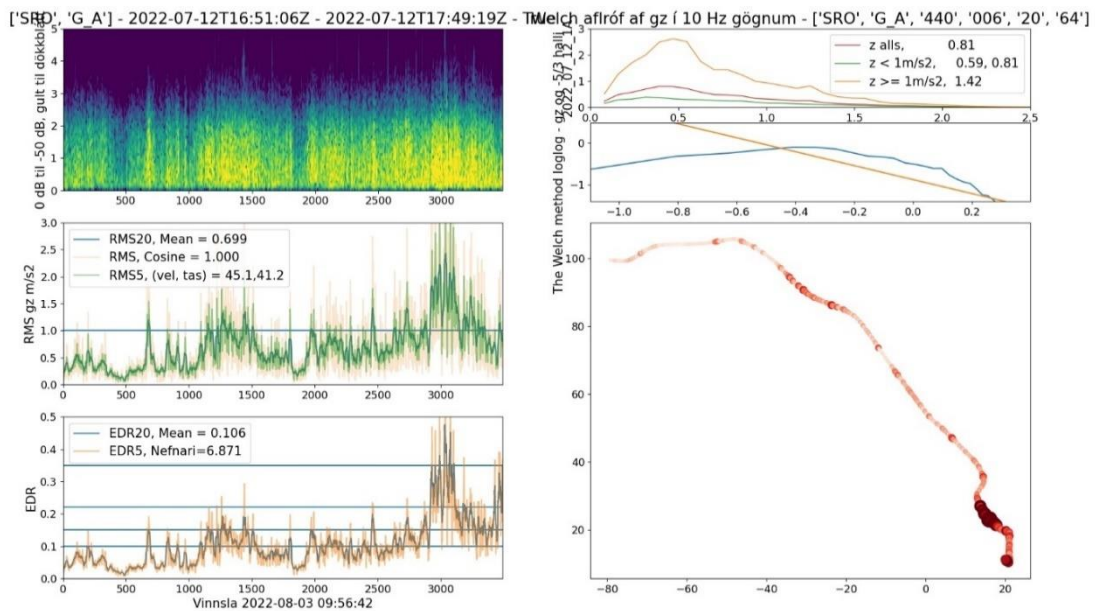


Figure 4-18 Flight Rif to Heiði. Coordinates in color graph in km from midpint in Hvassahraun.

The following table collects the range of various variables for 10 seconds surrounding the events, indicating variability in aircraft speed and the accelerations applying a rolling averaging window.

Table 4- 2. 10 seconds surrounding turbulent events.

<b>Turbulent events</b>	<b>12.07.2022</b>	
time s (+- 5s)	3042s	3080s
True airspeed m/s	30.4 to 37.1	25.4 to 36
Vertical speed m/s	-2.8 to 2.6	-4.1 to 0.8
Ground speed m/s	36.8 to 39	37.6 to 40.1
Peak acc m/s <sup>2</sup>	10.30	7.30
1s rolled m/s <sup>2</sup>	4.00	4.40
5s rolled m/s <sup>2</sup>	3.70	3.10
20s rolled m/s <sup>2</sup>	2.40	2.00
EDR5 m <sup>2/3</sup> /s	0.60	0.70
EDR20 m <sup>2/3</sup> /s	0.43	0.45

Variation in ground speed is relatively small compared to the variation in True Air Speed measured by Pitot (2 m/s vs 10 m/s) indicating the rapid change of indicated airspeed due to turbulence. Also notable is the variation in vertical aircraft velocity (5 m/s). The events resulted in similar EDR evaluations, yet one had a 10.3 m/s<sup>2</sup> (over 1 g) peak acceleration and the other event had a higher RMS value taken over 1 s. This shows in concrete examples the acceleration variability and relations between peak and rolling window averages.

#### 4.11 Proposed use of correlations and variability statistics

Correlation models can be used to generate an average EDR field in the vicinity of Hvasshraun and multipliers of 1.6 for 90th percentile, and 2.5 to 3 for peak values applied to represent peaks in EDR as discussed in Section 4.7. Therefore, EDR along any intended track can be evaluated. Readers are reminded that for the results below the model is applied for wind speeds outside its volume of correlation values, i.e. extrapolated.

As runways with the orientations of 14 and 04 have been proposed a situation will be generated for an aircraft profile with 5 degrees approach and departure angles along each runway direction with 20 m/s wind from 135 and 45 degrees respectively. The following table summarizes the results. The coordinates are specified in km from the center of the airport. The height of aircraft profiles starts at 600 m ASL upon entering the circle. The approach path is assumed to reach the midpoint at 60 m ASL with climb out with the same angle (5 degrees) as the approach. The most critical result is generated (higher EDR) for the 135 degrees wind. Apparently the highest 5s (20s values are almost the same) average EDR along these tracks is 0.28 (wind 135 degrees) at departing the area (5, -5, 425). An aircraft might at that point experience an EDR of more than 0.45 some 10 % of the time and occasional peaks exceeding 0.8. This would exceed the severe

EDR threshold of 0.35 for the Savannah aircraft. Looking up the values in Fig. 4-13 (chapter 4.9) would indicate occasional vertical average RMS acceleration for an approaching/leaving Savannah of  $4.5 \text{ m/s}^2$ , but only  $2 \text{ m/s}^2$  for an approaching Dash8-200 which would be considered moderate turbulence. This methodology can be used to look for EDR inhibiting values for different types of aircraft.

Table 4- 3 Approaching and departing aircraft

<b>Windspeed and direction: 20m/s, 135 degrees</b>				
<b>Correlation used: Case3, 5s EDR</b>			<b>EDR Mast est 0.37</b>	
Approach and departure at 5 degree angle				
Coordinate (km)	height(m)	EDR $\text{m}^{2/3}/\text{s}$	EDR*1.6	EDR*3
(-7,7)	600	0.135	0.22	0.41
(-3.5,3.5)	300	0.207	0.33	0.62
(0,0)	60	0.209	0.33	0.63
(3.5,-3.5)	300	0.272	0.44	0.82
(7,-7)	600	0.266	0.43	0.80
<b>Windspeed and direction: 20m/s, 45 degrees</b>				
<b>Correlation used: Case2, 5s EDR</b>			<b>EDR Mast est 0.25</b>	
Approach and departure at 5 degree angle				
Coordinate (km)	height(m)	EDR $\text{m}^{2/3}/\text{s}$	EDR*1.6	EDR*3
(-7,-7)	600	0.143	0.23	0.43
(-3.5,-3.5)	300	0.178	0.28	0.53
(0,0)	60	0.2	0.32	0.60
(3.5,3.5)	300	0.16	0.26	0.48
(7,7)	600	0.1	0.16	0.30

An alternative approach was presented in Section 4.6, that proposes to use the Mast 30 m EDR as a surrogate value for the highest EDR (5 s or 20 s average) that an aircraft might encounter in the area. For the case above the EDR value at the mast is 0.37, but highest value along the calculated track is 0.28. Using the mast value results in an expectation for the Savannah to hit occasionally 1 g acceleration (or severe turbulence). The Dash8-200 would be experiencing moderate turbulence (peak vertical acceleration significantly less than 1 g).

It should be noted that the proposed methodology for evaluating the utilization ratios (ísl - nothæfisstuðlar) for the airport, based solely on a turbulence criterion, should be conservative, especially in the high wind speed regime which has not been well explored by in-flight measurements. It should also be noted that the Met Mast is located only 1.5 km from the designated center of the airport. Consequently, it provides a continuous high-quality estimate of the mean EDR at 30 m height above the proposed airport site. Hence, it is a reliable and practically continuous measure of the low-level turbulence that an aircraft landing or taking off from runways at this location could experience.

If an airport is built in this location, airport authorities and aircraft operators will develop operating procedures for when and how to fly in the terminal airspace of the airport. At that time, more data will have been collected and experience in flying to/from the airport in various weather conditions will have been gathered.

## 5 Simulation of Aircraft Response to Typical Turbulence

The capability for simulating the response of an aircraft to the forces that act on it in turbulent air is essential for fully assessing the effect of this phenomenon that without exception disturbs the operation of air vehicles. Simulation was a key tool for developing the methods that have been applied to measure turbulence as discussed in the Pilot Project Report of this in-flight measurement project<sup>11</sup>. In this chapter the application of simulation for assessing the results of the measurement program is discussed. A key issue in this context is the use of the correlation models that have been developed in this project for describing the turbulent environment. Analysis of the response of the different types of aircraft likely to be operating at an airport in Hvassahraun as well as a quantitative approach for defining their operating boundaries are important aspects of this effort. Also, some potential further studies and research based on simulation of operational nature are discussed.

### 5.1 Objectives of the Simulations

The primary purpose of applying computer simulations in this project is to ascertain the effects of turbulence on various types of aircraft that are exposed to turbulence of the intensity expected in the Hvassahraun area. This is done by using the dynamic math models, that were applied for implementing in-situ measurements of vertical acceleration as described in the 2021 report (ref. 11), including the *de facto* standard simulation model for generating the vertical disturbance velocity. Thus, the response of aircraft of different types is reproduced under various turbulence conditions that have been observed and modeled through the program of in-situ measurements as described in Chapters 3 and 4. These measurements have led to the development of mathematical models of air turbulence in the airport area in terms of the internationally accepted metric of EDR intensity. These models are particularly well suited for assessing the performance of different types of aircraft operating in the area for given wind conditions measured at the met mast. Thus, the primary goal of the simulation in this project is to provide a comparison of aircraft accelerations for aircraft from the very light category to medium jet transports represented by the B 757. However, the simulator can be used for further analysis of the conditions in the area as is discussed further in Appendix H of this report.

It is submitted, that in addition to this primary purpose, it is also important to perform simulations to build further understanding and confidence in the methodology, which has been applied in the measurement and processing of the in-situ acceleration data. For example, the simulator provides a full frequency response history for the aircraft based on the low-frequency

---

<sup>11</sup> **Mælingar á loftkviku yfir Hvassahrauni – forverkefni jan-sept 2021;** (In-flight Measurements of turbulence over Hvassahraun Site – Pilot Project, Nov 2021)

correlation models. This response can be used to analyze the statistical effect on the aircraft for any flight profile within the modeled airspace. Thus, a flexible simulation capability of this type would be important for exploring operational procedures at other airports in Iceland assuming that more extensive EDR data is collected. More advanced aircraft dynamical models than the plunge model would be a valuable improvement in this context.<sup>12</sup>

## 5.2 Simulation Tool for Turbulence Assessment

The primary purpose of the simulator is to provide a tool for generating the dynamic response of an aircraft of a specified type to vertical air turbulence by computing the time histories of the vertical acceleration, velocity and other state variables of the aircraft as well as producing the driving disturbance i.e. the vertical turbulent wind component. The relatively simple simulator, which has been developed for this purpose, is made up of the components which are shown in Fig. 5-1:

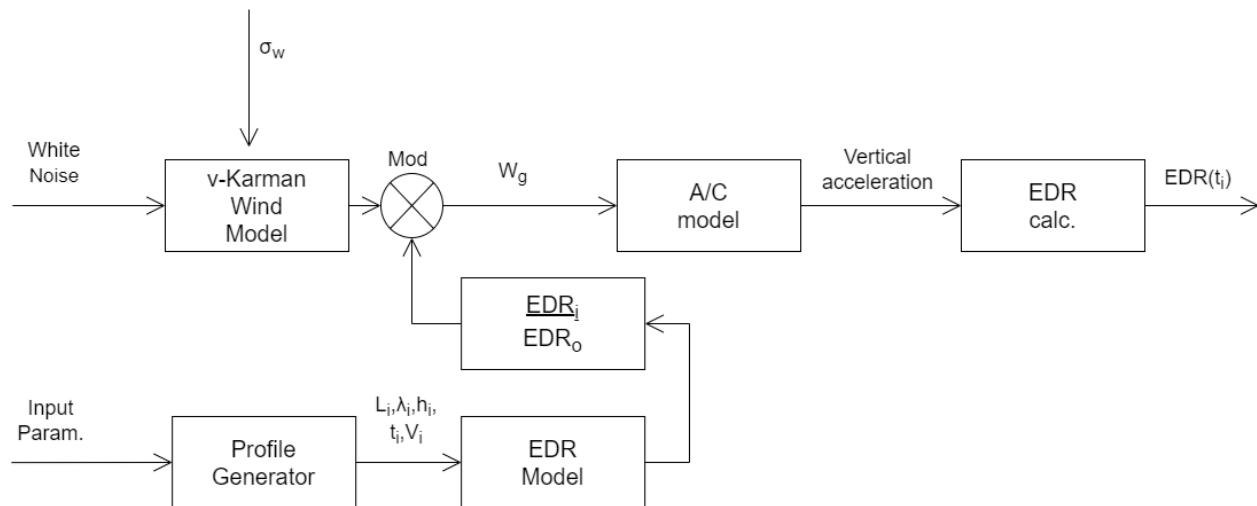


Figure 5-1. General configuration of the Turbulence Flight Simulator

The output that is of primary interest in this context is the vertical acceleration which, like all other simulated variables, is available as a function of time in high resolution. This is proportional to the load that is created by aerodynamic forces on the aircraft by the turbulent wind component acting on it. It also affects the occupants of the aircraft as well as loose items in its cabin. The fact that it can be made available for any given aircraft trajectory makes it ideal for determining the overall impact of a flight through the area for any given flight scenario. It is easy to ascertain the probability of peak loads and their duration if required. Variations or

<sup>12</sup> R.D. Sharman, L.B. Cornman, G. Meymaris, J. Pearson, and T. Farrar; **Description and Derived Climatologies of Automated In Situ Eddy-Dissipation-Rate Reports of Atmospheric Turbulence**, Journal of Applied Meteorology and Climatology, Vol. 53, January 2014

displacement from the flight path, which are important for flight path following such as required for a precision landing, can also be determined. However, this calls for a more complex aircraft model, which takes account of the pilot’s control efforts that can be manual or automatic. An important characteristic of the basic simulator model is that it is linear in nature. This means that doubling the signal strength results in a proportional increase of the output if no non-linear limitations are introduced. However, the modulation of the input signal, i.e. the vertical wind component introduces a nonlinearity. This is a straight-forward way of accounting for variations in EDR which are encountered and measured in the real-world environment. A more detailed description of the simulator and its application is provided in Appendix H and Appendix I of this chapter.

### 5.3 Response of Individual Aircraft types

The following simulation “tests” are conducted separately for each type of aircraft which are all in either the approach mode (final approach airspeed) or a typical Terminal Area maneuver airspeed (double final approach airspeed) as defined for the five types of aircraft considered in Table 5.1. Each “flight” is carried out for a constant turbulence EDR to generate the vertical windspeed value. No EDR modulation is applied in this case so that the simulation reaches steady-state conditions as the initial transients are not included. This value is in all the simulated tests chosen as  $EDR = 0.4 \text{ m}^{2/3}/\text{s}$  which is used for generating turbulent wind data to drive the simulation of the aircraft response in each case.<sup>13</sup> The output is primarily the acceleration level of each of these aircraft types at their specified airspeeds which are based on actual flight conditions during final approach at sea level and maneuvering at 2000 feet for each type. Subsequently, the ratios of the standard deviations of acceleration sequences are used for comparing the four types of aircraft considered in addition to the Savannah measurement aircraft which is by far the most responsive to air turbulence of the aircraft considered in this project. A rolling window of 20 seconds is used for all signal level RMS estimation calculations whereas estimates of standard deviations are obtained by averages taken over the full time periods of test runs.

Table 5.1 Specification of parameter values used for simulating aircraft responses for the five types of aircraft that would be expected to use Hvasshraun Airport.

Aircraft - configuration	Air density (kg/m <sup>3</sup> )	Mass (kg)	Air Speed (m/s)	Wing surface area (m <sup>2</sup> )	$\frac{dC_L}{d\alpha}$ (CL $\alpha$ ) (deg <sup>-1</sup> )	Mean chord length b (m)	Conversion Factor* (m <sup>1/3</sup> /s)	Bandpass filter window
Savannah final approach	1.225	450	30	12.9	4.77	1.4	5.1	0.1 – 2Hz
Savannah TA maneuver	1.225	450	60	12.9	4.77	1.4	9.8	0.1 – 2Hz
Dash 8-200 final approach	1.225	13,500	49	54.3	5.41	2.1	2.3	0.1 – 2Hz

<sup>13</sup> A.C. de Bruin, H. Haverdings; **Validation of an Eddy Dissipation Rate Calculation Method based on Flight Data Recording Data**, National Aerospace Laboratory Report NLR-CR-2007-540, December 2007.

Dash 8-200 TA maneuver	1.225	13,500	98	54.3	5.41	2.1	5.1	0.1 – 2Hz
King Air -200 final approach	1.225	4,673	50	28.2	5.22	1.7	3.2	0.1 – 2Hz
King Air -200 TA maneuver	1.225	4,673	100	28.2	5.22	1.7	6.8	0.1 – 2Hz
B737-9 final approach	1.225	61,000	71	127.0	5.25	4.6	1.9	0.1 – 2Hz
B737-9 TA maneuver	1.225	61,000	142	127.0	5.25	4.6	4.5	0.1 – 2Hz
B757-200 final approach	1.225	75,500	62	185.3	5.00	5.0	1.8	0.1 – 2Hz
B757-200 TA maneuver	1.225	75,500	124	185.3	5.00	5.0	4.2	0.1 – 2Hz

\* Conversion of EDR to standard deviation of vertical acceleration for a given type of aircraft and its operational specifications.

\*\* TA maneuver: maneuvering airspeed in Terminal Area

### 5.3.1 Response of Light Measurement Aircraft

The response of the primary measurement aircraft (Savannah/Ventura) is important as these aircraft have been used as the platforms for collecting most of the acceleration data. Clearly, they have the advantage of being very responsive to turbulence and hence are highly sensitive to the variable that is being evaluated. However, it is operationally limited in terms of the weather conditions for which it is suited. High and gusty wind at the airport limits their operation on the ground in mean wind-speed exceeding 20-25 m/s.

The response of the Savannah aircraft to a steady-state vertical wind component, set for EDR= 0.4 m<sup>2/3</sup>/s, is shown in Figure 5-2 a) in terms of (left to right): simulated aircraft vertical acceleration and vertical velocity. Randomly selected twenty second cut-outs are also shown to demonstrate in detail the high frequency variations of these variables. The vertical displacement of the aircraft from its intended flight path would require a more complicated aircraft model that included the way in which the aircraft altitude is controlled by the pilot, or more commonly auto-pilot, to maintain a desired level.

$$\text{EDR}=0.4 \text{ m}^{2/3}/\text{s}$$

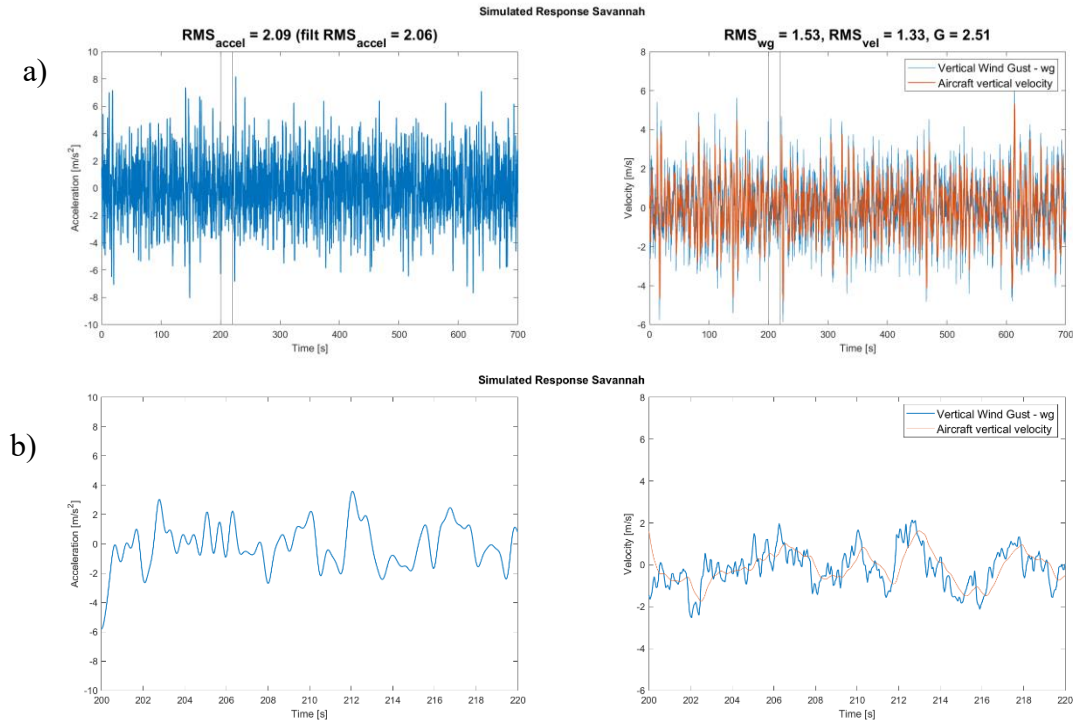


Figure 5-2. a) Simulated response of the Savannah aircraft at approach airspeed over a 700 second, 21 km flight segment. The vertical wind intensity is set for EDR = 0.4 resulting in vertical acceleration of RMS 2.06 m/s<sup>2</sup>. The corresponding RMS vertical speed of the wind is  $w_g = 1.53$  m/s resulting in vertical aircraft velocity of 1.33 m/s which is highly correlated with the vertical wind component; the acceleration reaches peak variations up to 6-7 m/s<sup>2</sup>, about 3x the RMS value. b) These provide 20 second cut-outs of the full simulation data record depicted to show the signal details from the simulator. The graphs show that the Savannah responds quickly to changes in vertical wind, albeit with a small phase-lag and slight attenuation of the higher frequencies (over 1 Hz).

The ratio of the vertical speed of the Savannah at approach airspeed is determined as:

$$\zeta = \hat{\sigma}_{vel}(\text{Sav}) / \hat{\sigma}_{wg}(\text{Sav}) = 1.33/1.53 = 0.87$$

where the “hat” over sigma denotes the computed average value of the standard deviation over the simulation run. This ratio and the vertical speed response shown in Figs 5-3 a) and b) demonstrate well how the light aircraft, with a low wing loading, is highly responsive to the turbulent vertical velocity component. Due to these properties the Savannah aircraft is in many ways an ideal reference for comparing the response of various types of aircraft.

The EDR estimation, obtained from the simulated acceleration series of the Savannah aircraft over a period of 700 seconds with an RMS window of 20 s, is shown in Fig. 5-3 as an example. Fluctuations in the order of plus or minus 0.1 to 0.15 are observed although the average value over the full period is almost precisely 0.4.

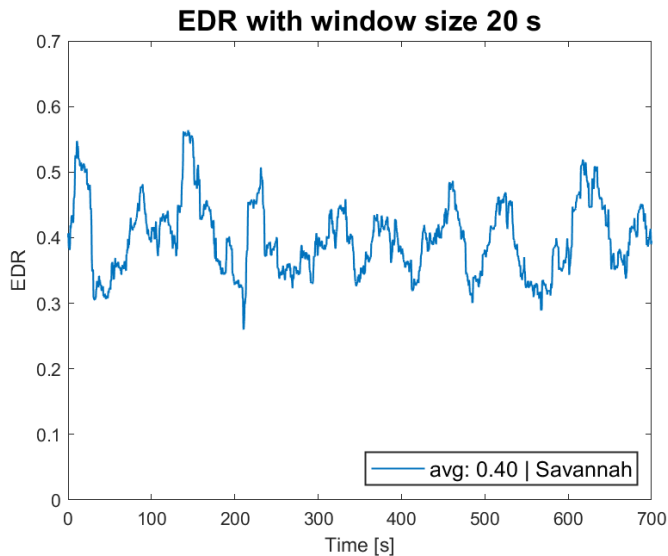


Figure 5-3 EDR obtained from the simulated acceleration of the Savannah aircraft.

### 5.3.2 Response of Bombardier Dash 8 – 200

The Bombardier Dash 8 – 200 is a typical regional aircraft in Iceland which is commonly used in inclement weather conditions with wind in the airport terminal area reaching 20-25 m/s. What follows in Fig. 5-4 is the simulated acceleration of the Dash 8 under the same conditions as were specified in the case of the Savannah aircraft. This means that the simulated vertical velocity has the same stochastic characteristics as that used in section 5.3.1. However, it is adjusted to the speed regime of the Dash 8. Similarly, the parameters of the aircraft response model are adjusted to appropriate values of the average airspeed, wing-loading and  $CL\alpha$  of the Dash 8.

$$\text{EDR}=0.4 \text{ m}^{2/3}/\text{s}$$

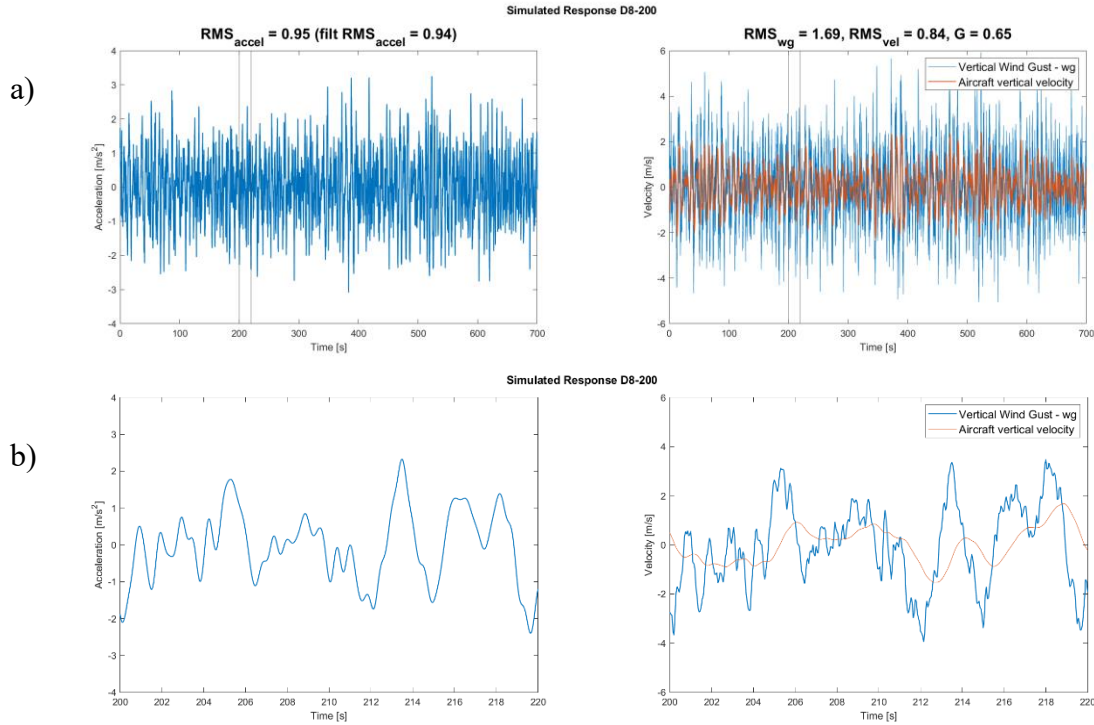


Figure 5-4. a) Response of the D8-200 aircraft at approach airspeed to a steady-state vertical wind intensity of  $\text{EDR}=0.4 \text{ m}^{2/3}/\text{s}$ , resulting in an RMS aircraft vertical acceleration of  $0.96 \text{ m/s}^2$ , RMS aircraft vertical speed of  $0.86 \text{ m/s}$ . Corresponding wind velocity is  $s_{wg} = 1.71 \text{ m/s}$ . The aircraft follows the the lower frequencies of the vertical wind component with a significantly lower amplitude and some slight time delay as can be seen from the more detailed cut-out of b) which contains a 20 second snippets of an 11-minute sequence of simulation history of 700 s. The RMS acceleration reaches peaks of  $3\text{-}4 \text{ m/s}^2$  at least  $3\times$  the RMS value.

The vertical acceleration characteristics of the Dash-8 in comparison with the Savannah is reflected by the ratio of the standard deviations of the two aircraft types to the same turbulence conditions as set up in the simulator:

$$\xi = \hat{\sigma}_{acc}(\text{D8}) / \hat{\sigma}_{acc}(\text{Sav}) = 0.94/2.06 = 0.46$$

Thus, the Dash 8 load response is about 47% of that of the Savannah as expressed by the ratio of standard deviations of vertical accelerations in the approach mode. The ratio between the vertical speed of the air and the aircraft are similarly determined as:

$$\zeta = \hat{\sigma}_{vel}(\text{D8}) / \hat{\sigma}_{wg}(\text{D8}) = 0.84/1.69 = 0.50$$

where the “hat” over sigma defines the estimated average value of the standard deviation of the period of simulation. The Dash 8 vertical speed response shown in Figs 5-3 a) and b) demonstrates how the larger and heavier aircraft, with significantly higher wing loading, does not respond to the high frequency of the disturbing vertical wind to the degree that is seen in the case of the ultra-light Savannah.

### 5.3.3 Response of Boeing 757-200

The Boeing 757-200 has been the mainstay of the Icelandair fleet for more than thirty years. Consequently, it represents an upper-end medium-sized jet transport which has over this time probably accumulated more hours of flight than any other type of transport aircraft on the Icelandic registry.

The results of the simulation of the flight of a B 757-200 through simulated air turbulence of the same type (i.e. in terms of turbulence intensity) as used in the case of the Savannah and Dash 8 is shown in figures 5-4 a) and b).

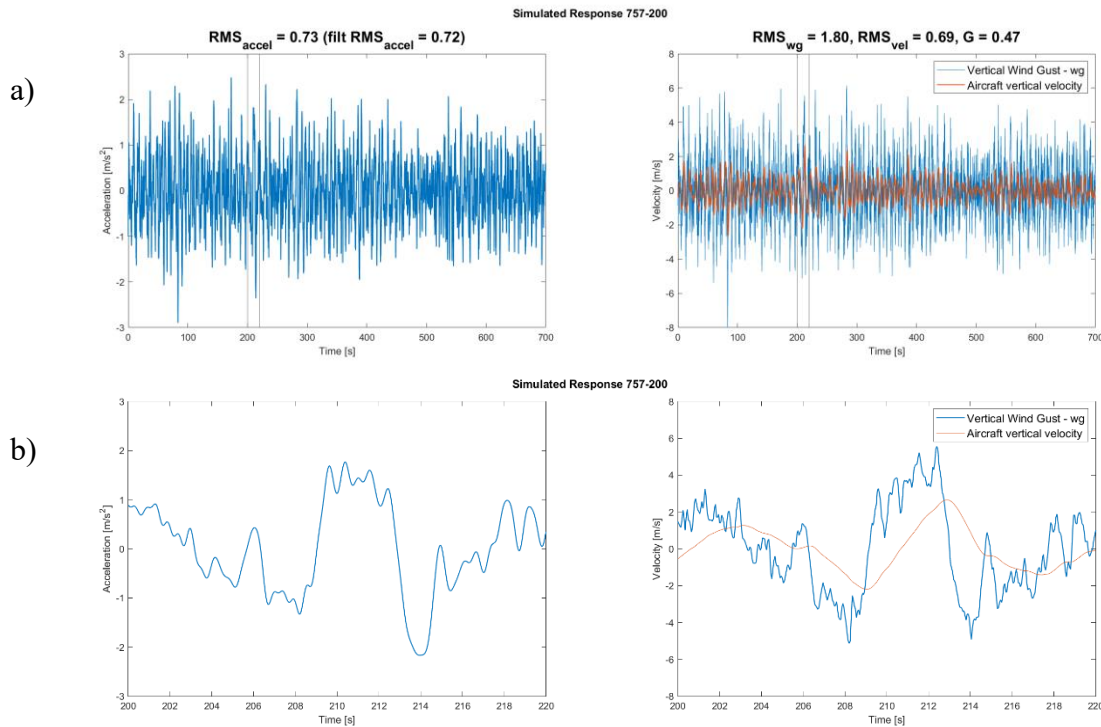


Figure 5-4 a) Response of the B757 aircraft to a steady-state vertical wind component set for  $w_g = 1.80$  m/s resulting in a vertical acceleration of RMS  $0.73$  m/s<sup>2</sup>. Note that the RMS vertical speed of the aircraft is about  $0.69$  m/s and is reasonably well correlated with the low-frequency vertical wind component. b) 20 second cut-out of the 2000-sec sequence of simulation data. The acceleration varies between the RMS bounds but reaches peaks of  $3$ - $3.5$  m/s<sup>2</sup> about  $3$ x the RMS value. The graphs clearly show that the B 757 with its high wing-loading is most sensitive to low-frequency changes in vertical wind.

The vertical acceleration characteristics of the Boeing 757-200 in comparison with the Savannah is reflected by the ratio of the standard deviation of the two aircraft types to the same turbulence conditions as set up in the simulator:

$$\xi = \hat{\sigma}_{acc} (\text{B757}) / \hat{\sigma}_{acc} (\text{Sav}) = 0.72/2.06 = 0.35$$

Thus, the B 757-200 load response in terms of the standard deviation of vertical acceleration is about 35% of that of the Savannah with both aircraft flying at their respective approach airspeeds. The ratio between the vertical speed of the air and the aircraft are similarly determined as:

$$\zeta = \hat{\sigma}_{vel}(B757) / \hat{\sigma}_{wg}(B757) = 0.69/1.80 = 0.38$$

where the “hat” over sigma,  $\hat{\sigma}$ , defines the estimated average value of the standard deviation over the period of simulation. The B 757-200 vertical speed response shown in Figs 5-4 a) and b) demonstrates how the larger and heavier aircraft, with much higher wing loading, does not respond to the high frequency of the disturbing vertical wind to the degree that is seen in the case of the ultra-light Savannah.

However, it does follow the much lower amplitude of the lower frequency disturbances. As mentioned before, the very low frequency disturbance would normally be alleviated by the pilot or autopilot who compensates for variations of attitude changes and maintains a level flight path. This is achieved by eliminating the turbulent wind below a frequency of 0.1 Hz by high-pass filtering. Thus, the focus remains on the inertial sub-range of frequencies.<sup>14</sup>

#### 5.3.4 Key Statistical Results of Type Simulation Tests

The response of an aircraft to turbulence is expressed primarily in terms of the standard deviation of the vertical acceleration with special attention to the peaks that are typical of this phenomenon. These metrics capture the most important component of turbulence that is routinely measured in commercial transport aircraft as a vital measure of operational load to analyze individual events as well as long term structural fatigue of the aircraft. In this project it is found convenient to use the ultra-light Savannah aircraft as a reference to express the relative sensitivity of other types of aircraft to turbulence. This provides a convenient measure of the sensitivity of various types of aircraft to vertical turbulence represented by the  $\xi$  - factor.

The results of the simulated turbulence tests of five types of aircraft, expected to operate at an airport in Hvassahraun, are provided in Tables 5.2 and 5.3 for the two airspeed regimes considered, i.e. final approach airspeed and twice that airspeed. These speeds vary in accordance with the specifications and performance of each type of aircraft. However, they all assume that the altitude is 2000 ft or less as reflected by the sea level air density as per Table 5-1, Description of simulated tests of two additional aircraft types given in the tables, i.e. the Beechcraft King Air 200 and B737-9, are provided in Appendices I. Thus, the aircraft types range from an ultralight aircraft, domestic ambulance aircraft, regional airliner, to two medium-sized jet transports. The application of the simulator, in conjunction with the turbulence models developed in this project, provides a useful

---

<sup>14</sup> A.C. de Bruin, H. Haverdings; **Validation of an Eddy Dissipation Rate Calculation Method based on Flight Data Recording Data**, National Aerospace Laboratory Report NLR-CR-2007-540, December 2007.

capability for analyzing in detail the response of different types of aircraft to either steady-state or variable intensity turbulence. These can be compared with the underlying turbulent wind which is output by the wind model simulation. The wind model, which approximates the standard von Karman model, is extensively used by the aviation industry as an accepted if not certified tool for describing the source of turbulence disturbances that cause aircraft to deviate from their intended trajectory of flight often referred to as aircraft profile. This data is not directly available from the acceleration measurements, which are commonly used for in-flight measurements.

Table 5.2 Response Characteristics of four types of aircraft to the same average EDR = 0.4 m<sup>2/3</sup>/s at typical final approach airspeeds as pr. Table 5-1.

Aircraft Type (A/C)	RMS A/C acceleration (m/s <sup>2</sup> )	RMS A/C acceleration (BP filtered)	RMS A/C velocity (m/s)	RMS wind vel. (m/s)	Xi* $\xi$	Zeta** $\zeta$
Savannah	2.09	2.06	1.33	1.53	1.00	0.87
D8-200	0.95	0.94	0.84	1.69	0.46	0.50
King Air 200	1.31	1.29	1.05	1.70	0.63	0.62
B737-9	0.80	0.79	0.77	1.94	0.39	0.40
B757-200	0.73	0.72	0.69	1.80	0.35	0.38

\*Xi -  $\xi$  is defined as the ratio of acceleration standard deviations:  $\sigma_{acc}(A/C) / \sigma_{acc}(Savannah)$  where A/C represents the aircraft type. \*\*Zeta -  $\zeta$  is the ratio of rms values of aircraft velocity and the wind velocity

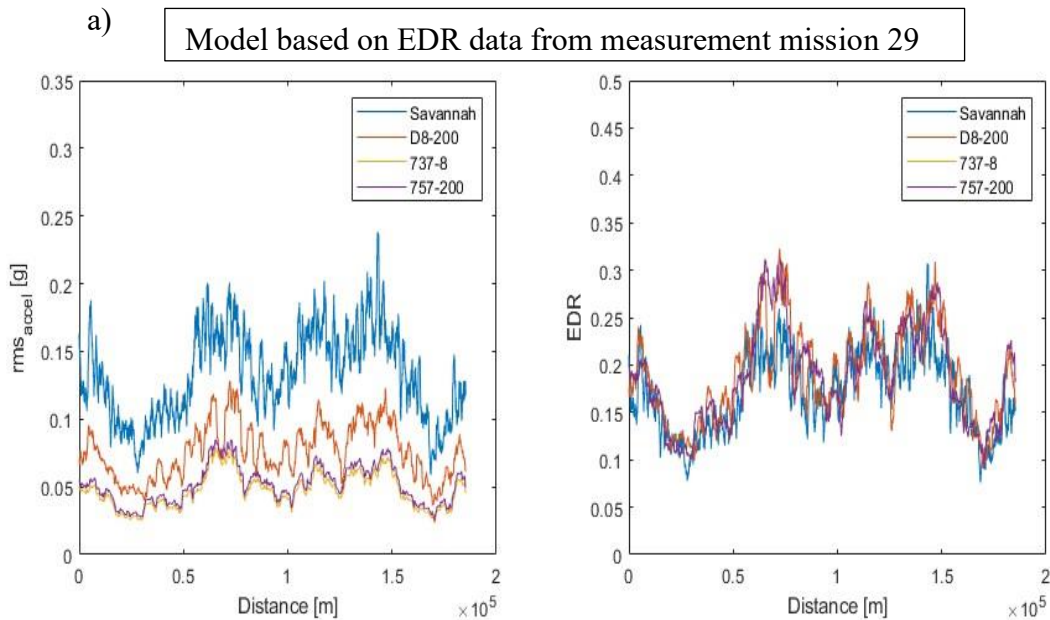
Table 5.3 Response Characteristics of five types of aircraft to the same average EDR = 0.4 m<sup>2/3</sup>/s but with double aircraft velocity representing a typical maneuvering airspeed in a Terminal Area as pr. Table 5-1.

Aircraft Type (A/C)	RMS A/C acceleration (m/s <sup>2</sup> )	RMS A/C acceleration (BP filtered)	RMS A/C velocity (m/s)	RMS wind vel. (m/s)	Xi* $\xi$	Zeta** $\zeta$
Savannah	4.14	3.91	1.90	2.04	1.00	0.93
D8-200	2.12	2.09	1.54	2.21	0.51	0.70
King Air 200	2.83	2.75	1.75	2.28	0.68	0.77
B737-9	1.85	1.82	1.50	2.44	0.45	0.61
B757-200	1.71	1.68	1.33	2.30	0.41	0.58

\*Xi -  $\xi$  is defined as the ratio of acceleration standard deviations:  $\sigma_{acc}(A/C) / \sigma_{acc}(Savannah)$  where A/C represents the aircraft type. \*\*Zeta -  $\zeta$  is the ratio of rms values of aircraft velocity and the wind velocity.

## 5.4 Comparative Response of Aircraft on a Fixed Course

The simulated responses for four types of aircraft on a fixed distance course are shown in Figs. 5-8 a) where the acceleration in terms of g's, is shown as a function of distance along a flight profile which was actually flown as a measurement flight on 29 Dec 2021 by the Savannah aircraft. The purpose of this exercise is to subject the different types of aircraft to the same pattern of turbulent wind disturbances over a fixed distance, in this case a typical mission over Hvassahraun. In the simulation the distance along the track is determined based on average cruising airspeed times the elapsed time. The duration of the slow measurement flight (Savannah aircraft) within the designated area was approximately one hour and a quarter. The flight times of the faster aircraft are correspondingly shorter dependent on the true airspeed selected for the simulation. The modulation of the turbulence strength is performed in this demonstration by using the EDR Case 1 model data reproduced by simulator following the actual recorded 3D measurement flight profile of the measurement aircraft. This is converted from spatial coordinates to the time domain for each aircraft type for carrying out the time-based simulation. Subsequently, EDR estimates, computed by using simulated vertical acceleration measurements, are recorded as a function of the along-track distance on a scale from 0 to 200 km. This provides a good indication of the consistency of the simulated data and a comparison of the results obtained from different types of aircraft.



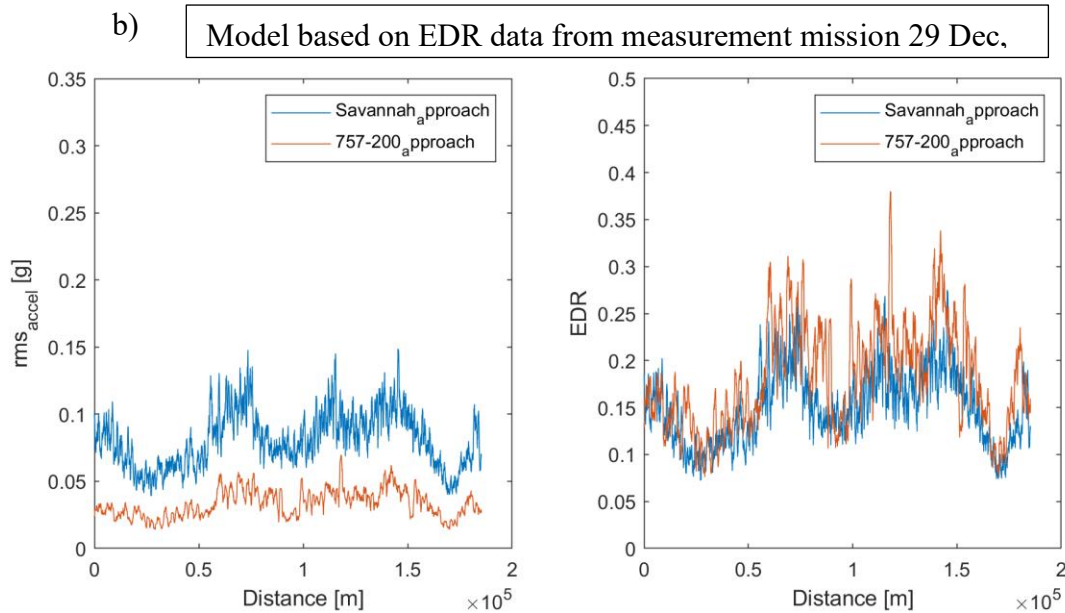


Figure 5-5. a) Simulated RMS acceleration and corresponding EDR estimates of four types of aircraft at cruising speeds based on simulated variable turbulence intensity measured on 29 Dec 2021 in the area over a 180 km distance or about 1:25 hours of Savannah flying time with a 20s rolling RMS window. B) Acceleration and EDR of Savannah and B 757-200 at approach airspeeds. EDR estimates are computed based on the simulated acceleration responses for two aircraft types with, respectively, the highest and lowest response levels of the types considered.

As seen in Fig. 5-5 a), the lightweight, low wing-loading Savannah (blue graph) responds most vigorously in acceleration to the approximately 0.17 EDR ( $m^{2/3}/s$ ) mean turbulence level. Thus, the ultra-light aircraft reaches an average level of 0.1g or about  $1 m/s^2$  and shows peaks of 0.23g or  $2.3 m/s^2$ , whereas a Boeing 757-200 is close to 0.04g or about  $0.4 m/s^2$  with peaks of  $0.8 m/s^2$ . Other types such as the Dash 8-200 and the B-737 fall in between the Savannah and B 757 which define the boundaries of this study as far as aircraft types are concerned.

The right-most graphs in Fig. 5-5 b) show the EDR estimates that are derived for approach airspeed for all four types of aircraft under the same turbulence conditions for the same flightpath. In other words, these are simulated measurements of vertical acceleration through the same wind field and the EDR estimates derived therefrom. The results for the four airplane types are very similar to the EDR history derived from the EDR correlation model. Surprisingly, the high frequency peaks of the B-757 tend to exceed those of the lightweight Savannah. However, the mean value of the EDR, exhibits rather small deviations from the estimates obtained from the simulated Savannah data. This demonstrates the universality of the EDR measure of turbulence intensity which is in theory independent of the type of aircraft used for measuring this quantity. Inaccuracies in the one-dimensional response models (plunge model) for the types of aircraft involved are possibly responsible to a large degree for the variations of EDR estimates derived from the simulated acceleration histories. The fact that the measurement rate is the same in all instances also affects the estimation accuracy of calculated EDR. As an example, an aircraft flying at twice the true

airspeed of the Savannah only collects half the number of measurements compared with the slow aircraft. Consequently, two-dimensional aircraft response models including pitch motion would most likely provide an improvement of the simulator performance especially for large aircraft which demonstrate sensitivity to pitch induced accelerations. The measurement rate could also be increased with increasing airspeed given the high bandwidth of the acceleration measurements now available from the solid-state sensors used in this project.

## 5.5 Simulations of Aircraft Response to Turbulence - Summary of Result

Two types of simulations, based on the models used for core processing of in-flight acceleration measurements, are described in this chapter. One involves general time-based testing of individual aircraft types to investigate their response to turbulence of specified intensity. This is performed in a classical manner by generating stationary vertical wind samples,  $w_g$ , that have a specified fixed intensity, i.e. a constant EDR value. The other type of test involves a more complex application of variable EDR (i.e. non-stationary) vertical wind conditions. These still satisfy the basic assumption of having a time-invariant frequency distribution of power despite slow changes of its intensity, i.e.  $\sigma_{wg}$  and EDR. This is implemented by modulation of the steady-state signal to avoid transient changes in the simulation models. Thus, real changes in turbulence intensity, that are always present in the real world are accommodated. According to Cornman (1995)<sup>15</sup> this is reasonable if the inhomogeneous variations result in low-frequency changes in the amplitude of the vertical wind component without variations of the distribution of its power spectrum.

The results of the time-based simulation tests, described in section 5.4, show that the response of the four classes of aircraft typically using Reykjavik Airport range from 1.0 for the Savannah (the reference aircraft) to 0.35 at approach airspeed and 0.41 at double this airspeed for the B 757-200 which is the least responsive of the five types of aircraft studied in this simulation analysis. Other types of aircraft considered in this report fall in between these values as seen in tables 5-2 and 5-3. This is expressed in terms of the ratio,  $\xi$ , of the standard deviations of vertical accelerations of the response of any specific type of aircraft divided by the standard deviation,  $\sigma_{accel.}$ , of the Savannah aircraft. Thus, the Savannah is used as the reference aircraft for this comparison.

This result is obtained by individually subjecting all simulated aircraft to the same EDR turbulence conditions as defined by the correlation models that are described in section 4.4 of this report. As the flight time over a fixed distance varies greatly according to airspeed the conditions of the estimated EDR vary as well. As the recording and sampling rates are the same for all runs the slowest aircraft, i.e. the Savannah, collects the most data which contributes to the quality of the results. Further details are presented in Appendices H and I of this report.

---

<sup>15</sup> L.B. Cornman, C.S. Morse and G. Cunnig; **Real-Time Estimation of Atmospheric Turbulence Severity from In-Situ Aircraft Measurements**, Journal of Aircraft Vol. 32, No. 1 January-February 1995

The overall conclusion drawn from the simulation tests is that there is general agreement between the outcome of the simulation tests, based on the use of EDR correlation models, and the conclusions drawn from the analysis of individual measurement missions. Hence, the simulations can be used to generate the results of aircraft loading (i.e. vertical acceleration) under various turbulence conditions on flight profiles that have not been flown by measurement aircraft. This can be achieved for any aircraft with an appropriate model of its dynamic characteristics that provides the response of the aircraft to a vertical wind described as a function of location and time. Operational studies based on Monte Carlo analyses could be easily performed by repeated simulation runs since the heavy computational requirements of such techniques do not present any major restriction given the computational performance of modern computers. The use of the simulator for undertaking comparative studies of two or more airports with respect to general turbulence conditions should also be noted. This would require the development of models of the type now available for Hvassahraun for other airports for comparison, i.e. the Reykjavik and Keflavik Airports. Such an effort can now be easily accomplished by applying the same measurement and processing techniques that have been developed in the Hvassahraun project. These can be carried out in a straight-forward way by use of dedicated aircraft as well as aircraft of opportunity during regular operations at the existing airports.

## 6 Conclusions and Recommendations

At the outset of the in-flight measurement program a pilot project was initiated to determine the feasibility of carrying out such measurements of air turbulence by using light aircraft equipped with relatively low-cost equipment. A report was submitted at the end of 2021 where the results of this pilot project and the measurement techniques are described. Moreover, a proposal was submitted for carrying out a program of measurements of vertical acceleration of the aircraft in an exploration area within 10 km from the center of the proposed Hvassahraun airport site, covering the main flight routes in its proximity. What followed were extensive and systematic measurement missions which were undertaken intermittently in 2022 and 2023. This chapter provides a summary of the project and its main conclusions that are drawn from the results of the measurement campaigns and studies carried out during the project and described in this report.

The main objectives of the in-flight measurement project as stated by the Ministry of Infrastructure are to:

1. *Express the results of the measurement program in a way that gives a clear picture of the frequency, intensity, and terrestrial distribution of air turbulence on aircraft operating in and out of the airport.*
2. *Describe the weather conditions, that create significant bumpiness in the air and could impair flight safety especially during take-off and landing as well as affecting usability of the airport.*
3. *Provide comparison of disturbance and discomfort of flight due to air turbulence over the new airport site as well as over the two neighboring airports at Keflavik and Reykjavik.*
4. *Assessment of how air turbulence affects various types of aircraft.*

It was understood that the first two objectives would be most demanding in terms of acquisition of measurement data which would have to be collected under a variety of weather conditions. Clearly the weather envelope of the small and light aircraft would be severely limited in windy weather and under Instrument Flight Rule (IFR) conditions. Much larger and heavier measurement aircraft would have to be secured for this purpose. However, the same flexible and autonomous measurement equipment could be used in this case. Furthermore, it was clear that the comparison of conditions at the three airports could only be carried out in a cursory manner since large scale in-flight measurements could not be collected for Keflavik and Reykjavik Airports without increased scope.

### 6.1 Summary and Results

From the outset of the in-situ measurement project it was decided, based on results of the pilot project, that the results of the turbulence measurements would be expressed in terms of the internationally acknowledged EDR intensity metric. This would be computed on the basis of

vertical acceleration measurements made by the airborne equipment especially developed for this purpose. The measurements would be recorded as a function of the aircraft position and time along the flight profiles defined in the Hvassahraun area and elsewhere as needed. This approach has the advantage of providing results which are independent of the type of aircraft used for taking the measurements and computing the EDR level. More importantly this can be applied to measurements collected by aircraft of different types whose dynamic characteristics are known.

Methods were also developed for transforming the measurements from each flight mission into EDR topographical charts within the primary area of investigation. This provides a convenient and easily accessible overview of the outcome of each measurement mission in two dimensions, i.e. the horizontal plane. The third dimension was added when measurements were recorded by three aircraft flying in the area at different altitudes at the same time. Thus, the third dimension was added opening the possibility of vertical sections to depict and demonstrate altitude dependence. The three-dimensional distribution is displayed by six graphic sections, four horizontal and two vertical ones, for each measurement mission as described in detail in Chapter 4 of this report.

As detailed analysis of measurement data in graphical and numerical terms from an increasing number of missions was carried out it was decided to concentrate the effort on three types of weather conditions. These were defined based on wind speed and direction at 30 m height of the specially installed Met mast. This instrumented mast is in the subject area within 1.5 km of the most likely center of the airport. These categories of weather conditions are as follows:

- a) Low wind conditions (below 5 m/s) in which case turbulence due to convection was expected to be prevalent - 6 flights.
- b) Wind directions between North to East (0-80 deg) with mean wind speed > 5 m/s - 11 flights.
- c) Wind directions between East to South (80-180 deg) and mean wind speed > 5 m/s - 12 flights.

The following conclusions are drawn based on the graphical mission data:

1. The convective turbulence in low wind strength conditions is weaker than expected and consequently deemed to be of little concern in this area.
2. Mean wind in the E-S sector of 8-9 m/s results in turbulence intensity on the EDR scale which is approximately 50% higher than wind of the same strength in the N-E sector.
3. With wind in the N-E sector the turbulence level in the airport area has a tendency to decrease with altitude.
4. With wind in the E-S sector the EDR turbulence level reaches a maximum at top of the mountain ridge at about 1000 feet (300 m). This is carried downwind from the ridge into the airport area.

In addition, correlation models were developed whereby estimates of mean EDR are generated for a given location and altitude above sea level for any point in the 10 km area given the wind speed and wind direction at 30 m height of the met mast (section 2.4). These models are used for determining the EDR turbulence intensity and resulting aircraft load in terms of vertical acceleration on any operational flight trajectory including approach and departure profiles. These are useful for drawing conclusions about the turbulence conditions in these and other aircraft operations within the area. Thus, it is concluded that:

1. The correlation models provide a realistic estimate of the average EDR level when compared with the measurements taken along the tracks of actual flights carried out by the measurement aircraft.
2. These models can be used for investigating the feasibility of using the EDR estimates obtained from the met mast wind measurements as a surrogate or proxy for the turbulence conditions in the area on a continuous basis.

Overall, the in-flight measurement data strongly suggests that the turbulence level, expressed in terms of EDR, increases with wind speed. Also, wind directions in the E-S sector result in significantly higher turbulence level than other wind directions for a given wind speed. These results are in conformance with general expectations and the measurements taken at the met mast. This outcome is supported by the concept that air turbulence in the area is made up of three main components i.e.:

- i. Turbulence transported into the area from afar, i.e. conditions outside the area.
- ii. Turbulence created when wind crosses the ridges and mountain tops on the edge of the area to the east and south of the airport site.
- iii. Turbulence created by wind interaction with rough terrain and lava fields within the area.

Based on these results turbulence in the E-S sector was investigated with the objective of determining wind speed and EDR conditions that would be likely to cause problems from a flight safety point of view. Analysis of all in-flight measurements that have been carried out reveal that if the Mast value is higher than 0.25, the 10 minutes mean EDR data recorded by the mast at the height of 30 m are always higher than the correlation EDR values estimated based on in-flight measurements taken elsewhere in the area (see fig 4-11). This is stated with the reservation that measurement flights have not been flown in strong wind conditions (wind speeds over 25 knots) which have to be carried out by heavier aircraft.

Thus, it is concluded that the EDR at the mast can be used as a surrogate or proxy for the highest mean EDR in the Hvassahraun airport area.

A total of twenty-nine missions were carried out over the Hvassahraun area. In a number of these missions the center of Reykjavíkflugvöllur was overflown at the same assigned flight level for performing turbulence measurements. In short, these measurements indicated that the level of turbulence was somewhat higher in Reykjavík when the wind direction was in the North to East ( $0^\circ - 80^\circ$ ) sector and vice versa for the East to South ( $80^\circ - 180^\circ$ ) sector. Only one flight with the Dash 8 aircraft was flown over Keflavík Airport in an 11 m/s wind from SSE which had a lower turbulence level than either Hvassahraun or Reykjavík.

Thus, it is concluded, albeit with limited data, that the turbulence level at Hvassahraun appears to be lower than that of Reykjavík Airport in northerly to easterly wind directions but more intensive in easterly to southerly wind directions than Reykjavík or Keflavík.

Given that EDR turbulence models are available for an airport area the acceleration- or g-loading of an aircraft can be estimated for all types of aircraft and flight paths and for different wind conditions. Furthermore, these can be assessed for different types of aircraft operating in different airspeeds regimes and aircraft weight which have a significant effect on aircraft response. The Savannah measurement aircraft is a logical example in this respect as it is highly sensitive to turbulence effects in all phases of flight. Its response for an EDR level of  $0.35 \text{ m}^{2/3}/\text{s}$  was found to cause approximately  $3 \text{ m/s}^2$  mean RMS vertical acceleration at cruising air speed (Fig 4-17 and section 4.9). This corresponds to  $10 \text{ m/s}^2$  or 1 g peak acceleration which would generally be considered “severe turbulence” indicating unsafe conditions for this type of light aircraft. Reduced airspeed in approach mode would lower this value closer to  $2 \text{ m/s}^2$  which would be termed as “moderate turbulence”. It should be noted that in accordance with the correlation models the EDR value at the 30 m mast height exceeds 0.35 in SE wind direction at a windspeed of 18 m/s. This is above the stall speed of the aircraft and would be considered unadvisable or unsafe for operation of this type of aircraft on the ground or in the air. Clearly, high wind speed, turbulence and wind gusts all contribute to prevent safe operation of light aircraft in these conditions.

Passengers in Dash 8-200 type of aircraft approaching and taking off under these conditions would experience “moderate turbulence” at EDR value of 0.7-0.8. This corresponds to a wind speed of approximately 30 m/s at the height of the 30 m high mast. The Met Office Report<sup>16</sup> will indicate how frequently such wind condition may occur. In accordance with the correlation models developed in this project “severe turbulence” for this type of aircraft does not arise until the EDR values exceed 1.0. Even higher values define this boundary for aircraft in the B 737 and B 757 class of medium transport aircraft.

In this context it is important to note that in-flight measurement flights have not been carried out in wind conditions over 12 m/s in the Hvassahraun area. It is essential that this is rectified in the coming months to broaden the validation envelope of the EDR correlation models. It is also worth noting that turbulence measurements of the type described here do not provide information

<sup>16</sup> Skýrsla Veðurstofu Íslands ; (titill) feb 2024

on wind shear at low level (< 100m height), i.e. spatial variations of mean wind speed due to obstructions near the airport, natural and man-made.

It is concluded, based on these results, that an EDR value of 0.4 at the 30 m mast, would most likely impede or curtail the operation of small/light aircraft in the Hvassahraun area. However, such turbulence by itself would not hamper the operation of Dash 8 aircraft or larger transport aircraft although moderate turbulence is likely to be experienced by the larger aircraft for EDR higher than 0.5-0.6 at the 30 m mast.

## 6.2 Main Conclusions

### 6.2.1 Turbulence frequency, strength, and geographic distribution

Through multi-linear correlations it has been possible to establish a connection between EDR in the Hvassahraun area with mast measurements of general wind conditions, i.e. wind speed and wind direction. The results are condensed into the correlations using least-squares methods that describe the geographic distribution of EDR as well as its strength with wind speed and direction. The frequency of certain levels of EDR can be deduced from the wind rose for the area as published by the Icelandic Met Office. This means that the wind rose of the mast can be used to estimate frequency of EDR exceeding certain values in various locations within the area of interest.

### 6.2.2 Weather influence of turbulence on airport safety and utilization

The analysis of in-flight measurements has demonstrated that EDR (indication of the intensity of turbulence) in the Hvassahraun area is a strong function of the wind speed. Furthermore, influenced by the wind direction it is unevenly distributed in the area of interest. We have further demonstrated that conditions that will generate severe turbulence for some aircraft will occur. We have a model (correlation) that allows for estimating EDR for given windspeed and direction along a chosen track, for example for landing or go-around, and this can be compared to calculated tolerance limit (for example severe turbulence) for different aircraft.

### 6.2.3 Comparison of Keflavik and Reykjavik Airports with Hvassahraun Site

Most of the in-flight measurement missions have been focused on Hvassahraun. Some of these flights have passed over Reykjavík Airport based on opportunity to collect turbulence measurements for comparison. In general, there is not much difference between the two sites (see section 3.2). However, it should be noted that no such visits have occurred in extreme weather conditions. Also, the vicinity of Reykjavik Airport has not been explored to the extent of the Hvassahraun area. The only pass over Keflavik Airport in a southerly wind direction and moderate wind speed indicated lower turbulence levels than in Hvassahraun and Reykjavik at that point in time.

#### 6.2.4 Effect of turbulence on various types of aircraft

Simulations show that EDR sensitivity varies greatly between aircraft types and whether the aircraft are in cruising mode (above the maneuvering speed) or flying at approach speeds. The ratio of standard deviation of acceleration provides a convenient if simple comparison of the response of the various classes of aircraft. These vary from 1.0 for very light aircraft such as the Savannah to 0.4 for medium size jet transports of the B 757 size. The Dash 8-200, a regional turbojet transport, falls in between these two with a value of approximately 0.6 whereas the outcome for a Beechcraft B-200 is about 0.7. Thus, the sensitivity to turbulence of the various classes of aircraft varies significantly. Also, the response is significantly affected by indicated airspeed and aircraft weight as discussed in sections 1.3 and 1.6 of this report.

### 6.3 Recommendations

#### 6.3.1 Further analyses and studies

Numerous further analyses of the turbulence conditions at Hvasshraun and for that matter the two neighboring airports at Reykjavik and Keflavik could be undertaken by more extensive application of the tools and methods developed and described in this report. Most prominent are the following:

- > Further application of the turbulence models already developed for exploring specific operations in the airport area of Hvasshraun using simulation and other quantitative methods and metrics.
- > Development of similar models for Reykjavik and Keflavik Airports and a thorough comparison of the turbulence conditions at the three airport sites already addressed in this report. This would require some further in-flight measurements to be undertaken and consultation aviation stakeholders.
- > Improvement of aircraft simulation models for assessing turbulence loading of aircraft different types by application of two-degree of freedom models to estimate the response of aircraft to recorded turbulence more accurately.

#### 6.3.2 Further research

- > Further refinements of the models and modeling techniques developed in this project. As an example, the correlation of turbulence and the wind conditions derived from multiple sources (e.g. ground based wind masts and wind forecasts) could be interesting for this purpose.
- > Methods for collecting turbulence data from aircraft in regular operation in Iceland would be of great importance for developing better tools for assessing turbulence conditions at

airports and on air-routes in Icelandic airspace. A data network based on use of the public GSM system has already been developed to a prototype level in the project described in this report.

- > Research of the turbulence environment at low levels in Icelandic airports to gain a better understanding of wind shear and turbulence under severe wind conditions and other extreme weather phenomena.